Agenzia nazionale per le nuove tecnologie, l'energia e lo sviluppo economico sostenibile

MINISTERO DELLA TRANSIZIONE ECOLOGICA

Documento di sintesi del piano di comunicazione e disseminazione - II anno

M. Valenti, G. Adinolfi, R. Ciavarella,
A. Merola, V. Palladino, A. Ricca

RdS/PTR(2020)/008

DOCUMENTO DI SINTESI DEL PIANO DI COMUNICAZIONE E DISSEMINAZIONE - II ANNO

M. Valenti (ENEA), G. Adinolfi (ENEA), R. Ciavarella (ENEA),
A. Merola (ENEA), V. Palladino (ENEA), A. Ricca (ENEA).

Aprile 2021

Report Ricerca di Sistema Elettrico

Accordo di Programma Ministero della Transizione Ecologica - ENEA
Piano Triennale di Realizzazione 2019-2021 - II annualità
Obiettivo: Sistema Elettrico
Progetto: *2.7 Modelli e strumenti per incrementare l'efficienza energetica nel ciclo di produzione, trasporto, distribuzione dell'elettricità*
Work package: *Analisi delle problematiche di gestione per l'integrazione nelle attuali reti in AC di nuove reti in DC in MT/BT (Media Tensione/Bassa Tensione)*
Linea di attività LA1.11: *Comunicazione e disseminazione 2*
Responsabile del Progetto: Maria Valenti, ENEA

Indice

Sommario

Le attività di disseminazione condotte nell'ambito della LA1.11 sono state preparatorie rispetto ad eventi e articoli pubblicati nel corso della terza annualità. Più nello specifico, si sono intraprese sia azioni volte a disseminare i risultati del progetto verso una platea più ampia che non comprendesse solo la comunità scientifica (azioni di comunicazione), sia azioni che consentissero una divulgazione più specialistica rivolta alla comunità scientifica (azioni di divulgazione scientifica). In relazione alle prime, si è proceduto ad organizzare un ciclo di seminari tematici in collaborazione con il progetto ESPA dell'ENEA e si è provveduto a selezionare eventi sul tema di interesse del progetto 2.7. In merito alla divulgazione scientifica si è intrapresa l'organizzazione di una special session nell'ambito della conferenza internazionale EEEIC 2021. In parallelo, i diversi partner di progetto hanno avviato la fase di redazione degli articoli di disseminazione scientifica. In sintesi, le attività condotte hanno riguardato:

- Organizzazione della special session "Reliability and energy efficiency issues in DC and hybrid AC/DC microgrids" nell'ambito della Conferenza Internazionale EEEIC 2021 on Environment and Electrical Engineering.
- Organizzazione di un ciclo di 4 seminari tecnici sul tema dell'affidabilità delle reti elettriche ibride AC/DC.
- Preparazione di 7 articoli scientifici da sottomettere alla special session "Reliability and energy efficiency issues in DC and hybrid AC/DC microgrids" nell'ambito della Conferenza Internazionale EEEIC 2021 on Environment and Electrical Engineering.

1 Organizzazione Ciclo di Seminari

Nell'ambito delle attività della LA1.11, è stato organizzato un ciclo di seminari di tipo divulgativo da erogare nel corso del III SAL. Le attività di tipo organizzativo condotte sono di seguito sintetizzate.
Data la natura divulgativa dell'evento e la necessità di coinvolgere una platea più ampia della sola comunità scientifica, il ciclo di seminari è stato organizzato in collaborazione con il progetto ES-PA[1] (Energia e Sostenibilità per la Pubblica Amministrazione) e di concerto con l'Ufficio Comunicazione dell'ENEA. Il ciclo di seminari è stato pianificato su quattro giornate con interventi tecnico scientifici relativi ad entrambi i progetti e con focus specifico sulle tematiche delle Smart Grid e delle Fonti Rinnovabili (progetto ES-PA) e dell'affidabilità delle reti ibride MT/BT per la divulgazione del progetto 2.7 di Ricerca di Sistema. In relazione al progetto 2.7, di concerto con le università, si è pianificato di far intervenire un diverso partner per ciascuna giornata così da illustrare le attività condotte e i risultati ottenuti in relazione alle specifiche LA. Alla luce di tale decisione, sono stati fissati temi, relatori e date degli interventi e costruite le locandine riportate di seguito. Per l'erogazione dei seminari si è deciso di procedere utilizzando la "modalità webinar" per le problematiche connesse alla pandemia e di rendere altresì disponibili le registrazioni dei video via YouTube sul canale dell'ENEA. Successivamente, sono stati fissati i canali di promozione del ciclo di seminari e le date (aprile – settembre 2021) in cui attivare le azioni di invito alla partecipazione. Al fine di coinvolgere il maggior numero di partecipanti dai diversi settori, si è deciso di utilizzare i seguenti canali di promozione: sito istituzionale ENEA, canale YouTube ENEA Eventi, newsletter ENEAinform@, sito Progetto ES-PA (per il coinvolgimento degli addetti delle Pubbliche Amministrazioni) e account ENEA sulla piattaforma online LinkedIn.
Le locandine predisposte sono di seguito riportate.

[1] https://www.espa.enea.it/

UNIONE EUROPEA

ENEA

PON GOVERNANCE E CAPACITÀ ISTITUZIONALE 2014-2020

LE SMART GRID PER UN FUTURO PIU' GREEN

21 aprile 2021
14.00 - 16:00

Il Programma Operativo Nazionale Governance e Capacità Istituzionale è il principale strumento della politica di coesione 2014-2020 dell'Unione europea per attuare le priorità strategiche in materia di rafforzamento e innovazione della Pubblica Amministrazione. In quest'ottica il Programma ha finanziato il Progetto dell'ENEA "Energia e Sostenibilità per la P.A." (ES-PA), che mira ad un rafforzamento delle competenze dei pubblici amministratori sui temi energetici e della sostenibilità.
Nell'ambito del Progetto, il Technology Brief sulle Smart Grid, predisposto da ENEA, fornisce una panoramica delle caratteristiche tecniche e dello stato di sviluppo tecnologico delle smart grid in ambito nazionale e internazionale, ponendo particolare attenzione alle soluzioni tecnologiche innovative smart a supporto di reti energetiche intelligenti che consentano una maggiore integrazione di fonti rinnovabili preservando disponibilità, sicurezza ed affidabilità.

ES PA ENERGIA E SOSTENIBILITÀ PER LA PUBBLICA AMMINISTRAZIONE

In collaborazione con:

RICERCA DI SISTEMA ELETTRICO
Accordo di Programma MISE-ENEA

PROGRAMMA

14.00 Saluto di benvenuto e apertura dei lavori
- Viviana Cigolotti, ENEA

14.10 Il Progetto ES-PA per le Pubbliche Amministrazioni locali
- Viviana Cigolotti, ENEA

14.30 Technology Brief sulle Smart Grid
- Maria Valenti, ENEA

15.00 Le problematiche di affidabilità nelle reti ibride di distribuzione
- Giovanna Adinolfi, ENEA

15.30 Question Time

16.00 Conclusioni

Figura 1 –Locandina primo seminario 2021

UNIONE EUROPEA
Fondo Sociale Europeo
Fondo Europeo di Sviluppo Regionale

Agenzia per la Coesione Territoriale

ENEA
Agenzia nazionale per le nuove tecnologie, l'energia e lo sviluppo economico sostenibile

PON GOVERNANCE E CAPACITÀ ISTITUZIONALE 2014-2020

TECNOLOGIE PER L'EFFICIENTAMENTO E LA GESTIONE OTTIMIZZATA DELLE RETI ENERGETICHE INTEGRATE

Venerdì 4 giugno 2021 | ore 10.00-11.30

ES PA ENERGIA E SOSTENIBILITÀ PER LA PUBBLICA AMMINISTRAZIONE

Il Programma Operativo Nazionale Governance e Capacità Istituzionale è il principale strumento della politica di coesione 2014-2020 dell'Unione europea per attuare le priorità strategiche in materia di rafforzamento e innovazione della Pubblica Amministrazione. In quest'ottica il Programma ha finanziato il Progetto dell'ENEA "Energia e Sostenibilità per la P.A." (ES-PA), che mira ad un rafforzamento delle competenze dei pubblici amministratori sui temi energetici e della sostenibilità.
Nell'ambito del Progetto, il Technology Brief sulle tecnologie energetiche per l'efficientamento e la gestione ottimizzata delle reti energetiche integrate, predisposto da ENEA, fornisce una panoramica delle caratteristiche principali delle reti energetiche integrate con una rassegna critica delle tecnologie più significative per l'efficientamento e la gestione ottimizzata di tali sistemi in presenza di poligenerazione distribuita da fonte rinnovabile e non, e sistemi di accumulo elettrico e termico.
Il presente documento si colloca nell'ambito dell'Attività 1.6.2 del Progetto ESPA che si pone come obiettivo il miglioramento della pianificazione energetica regionale nel settore della produzione da fonte rinnovabile e delle reti energetiche.

In collaborazione con:

RICERCA DI SISTEMA ELETTRICO
Accordo di Programma MISE-ENEA

PROGRAMMA

10.00 **SALUTO DI BENVENUTO E APERTURA DEI LAVORI**
Marialaura Di Somma, ENEA

10.10 **TECNOLOGIE PER L'EFFICIENTAMENTO E LA GESTIONE OTTIMIZZATA DELLE RETI ENERGETICHE INTEGRATE**
Marialaura Di Somma, ENEA

10.40 **SCENARI ENERGETICI ED EVOLUZIONE DELLE RETI ELETTRICHE DI DISTRIBUZIONE**
Salvatore Favuzza e Gaetano Zizzo, Università degli Studi di Palermo

11.10 **QUESTION TIME**

11.30 **CONCLUSIONI**

Figura 2 Locandina secondo seminario 2021

UNIONE EUROPEA
Fondo Sociale Europeo
Fondo Europeo di Sviluppo Regionale

Agenzia per la Coesione Territoriale

ENEA
Agenzia nazionale per le nuove tecnologie, l'energia e lo sviluppo economico sostenibile

PON GOVERNANCE E CAPACITÀ ISTITUZIONALE 2014-2020

STRUMENTI DI ANALISI ECONOMICO/AMBIENTALE DELLE STRATEGIE DI GESTIONE DI RETI ENERGETICHE INTEGRATE

Venerdì 25 giugno 2021 - ore 10.00-11.30

ES-PA ENERGIA E SOSTENIBILITÀ PER LA PUBBLICA AMMINISTRAZIONE

Il Programma Operativo Nazionale Governance e Capacità Istituzionale è il principale strumento della politica di coesione 2014-2020 dell'Unione europea per attuare le priorità strategiche in materia di rafforzamento e innovazione della Pubblica Amministrazione. In quest'ottica il Programma ha finanziato il Progetto dell'ENEA "Energia e Sostenibilità per la P.A." (ES-PA), che mira ad un rafforzamento delle competenze dei pubblici amministratori sui temi energetici e della sostenibilità.
Nell'ambito del Progetto, è stato realizzato da ENEA uno strumento di analisi economico/ambientale delle strategie di gestione di reti/microreti energetiche caratterizzate dalla presenza di impianti di poligenerazione distribuita e fonti rinnovabili elettriche e termiche, che consente di determinare il costo energetico totale giornaliero e la quantità totale di emissioni di CO_2 giornaliere relative alle strategie di gestione adottate per il funzionamento della rete/microrete energetica in esame. Tale strumento si rivolge alla Pubblica Amministrazione allo scopo di migliorare la pianificazione energetica regionale nel settore della produzione da fonte rinnovabile e delle reti energetiche, consentendo di effettuare una valutazione tecnico-economica e ambientale delle diverse strategie/soluzioni adottabili nell'ambito di reti/microreti energetiche.
Il presente documento si colloca nell'ambito dell'Attività 1.6.3 del Progetto ES-PA, che si pone come obiettivo il miglioramento della pianificazione energetica regionale nel settore della produzione da fonte rinnovabile e delle reti energetiche.

PROGRAMMA

10.00 **SALUTO DI BENVENUTO E APERTURA DEI LAVORI**
Marialaura Di Somma, ENEA

10.10 **STRUMENTI DI ANALISI ECONOMICO/AMBIENTALE DELLE STRATEGIE DI GESTIONE DI RETI ENERGETICHE INTEGRATE**
Marialaura Di Somma, ENEA

10.40 **LOGICHE DI GESTIONE ENERGETICA DI UNA RETE IBRIDA PROPRIETARIA PER L'ALIMENTAZIONE DI SISTEMI DI MOBILITÀ**
Giovanni Lutzemberger, Università di Pisa

11.10 **QUESTION TIME**

11.30 **CONCLUSIONI**

In collaborazione con:

RICERCA DI SISTEMA ELETTRICO
Accordo di Programma MISE-ENEA

Figura 3 Locandina terzo seminario 2021

IL RUOLO DELLE RETI IN CORRENTE CONTINUA E SMART NEI FUTURI SCENARI ENERGETICI

Lunedì 27 settembre 2021 - ore 10.00-11.30

ENERGIA E SOSTENIBILITÀ PER LA PUBBLICA AMMINISTRAZIONE

Il Programma Operativo Nazionale Governance e Capacità Istituzionale è il principale strumento della politica di coesione 2014-2020 dell'Unione europea per attuare le priorità strategiche in materia di rafforzamento e innovazione della Pubblica Amministrazione. In quest'ottica il Programma ha finanziato il Progetto dell'ENEA "Energia e Sostenibilità per la P.A." (ES-PA), che mira ad un rafforzamento delle competenze dei pubblici amministratori sui temi energetici e della sostenibilità.
Nell'ambito del Progetto, il Technology Brief sulle Linee guida sul quadro regolatorio e normativo delle Smart Grid, predisposto da ENEA, fornisce una panoramica sul quadro regolatorio e normativo e sullo stato di sviluppo tecnologico delle smart grid in ambito nazionale e internazionale, ponendo particolare attenzione alle soluzioni tecnologiche innovative smart a supporto di reti energetiche intelligenti che consentano una maggiore integrazione di fonti rinnovabili preservando disponibilità, sicurezza ed affidabilità.

PROGRAMMA

10.00 **SALUTO DI BENVENUTO E APERTURA DEI LAVORI**
Maria Valenti, ENEA

10.10 **LINEE GUIDA SUL QUADRO REGOLATORIO E NORMATIVO DELLE SMART GRID**
Salvatore Fabozzi, ENEA

10.40 **I VANTAGGI DELLE RETI IN CORRENTE CONTINUA NELL'AMBITO DELLA TRANSIZIONE ENERGETICA VERSO TECNOLOGIE SOSTENIBILI**
Morris Brenna, Politecnico di Milano

11.10 **QUESTION TIME**

11.30 **CONCLUSIONI**

In collaborazione con:

RICERCA DI SISTEMA ELETTRICO

Figura 4 Locandina quarto seminario 2021

2 Special session - Conferenza EEEIC 2021

In piena complementarità con l'azione divulgativa mirata a raggiungere un più ampio target di stakeholder, si è intrapresa un'azione di divulgazione mirata al raggiungimento della comunità scientifica da erogarsi nel corso della terza annualità di progetto (SAL 2021). In tal senso, nel corso del SAL 2020, si è organizzata una special session sul tema delle problematiche di affidabilità nelle reti elettriche DC e ibride AC/DC, ovvero con focus sulla tematica specifica del progetto 2.7 all'interno della conferenza internazionale International Conference on Environment and Electrical Engineering (EEEIC 2021). Nel corso del 2020, si è, quindi,

proceduto a definire un abstract illustrativo della special session (obiettivi, titolo e topic ammessi) da sottoporre, per l'approvazione, al Comitato Scientifico della conferenza. I dettagli relativi alla Special Session sono di seguito riportati nella locandina dell'evento stesso.

SPECIAL SESSION

Reliability and energy efficiency issues in DC and hybrid AC/DC microgrids

---

ORGANIZED AND CHAIRED BY:
Maria Valenti (ENEA, Italy)

CONTACT EMAIL:
maria.valenti@enea.it

OBJECTIVE AND TOPICS:

Distribution grids are evolving including new technologies, ICT, power electronics and so on. In this transformation, two key factors must only be taken into account: reliability and energy efficiency. New grid models must as reliable as the traditional ones or, if possible, assure an higher level of security of supply. Moreover, they must provide efficient ways for exploiting the energy resources connected to their nodes, such as renewables, energy storage systems and so on. These issues become more and more important if we consider the possibility that whole portions of the utility distribution grid could become DC or hybrid AC/DC microgrids, creating a new systems using components and devices whose reliability is still not tested in the filed like those for traditional AC systems.

In this context, the special session accepts papers on the issue of reliability and energy efficiency in DC and hybrid AC/DC microgrids. A non-exhaustive list of topics is reported below:

1. **Reliability in LVDC and MVDC microgrids;**
2. **Reliability and energy efficiency in DC and hybrid AC/DC microgrids;**
3. **Case studies of microgrids with DC components and devices;**
4. **Future energy scenarios and their impact on DC technologies penetration in distribution grids;**
5. **Distributed DC resources;**
6. **Protection of DC and hybrid AC/DC microgrids;**
7. **Energy management systems for hybrid AC/DC microgrids.**

Figura 5 Special session Conferenza EEIC 2021

3 Articoli di disseminazione scientifica

Nel corso del SAL 2020 si è proceduto a predisporre la stesura di sette articoli (3 ENEA, 2 Università di Palermo, 1 Università di Pisa, 1 Università di Milano) da sottomettere alla Special Session della conferenza EEEIC 2021, la cui deadline di consegna del full paper (preliminary submission) era prevista per il primo trimestre 2021. Di seguito si riportata l'elenco delle pubblicazioni dei 7 articoli redatti nel corso del SAL 2020, di cui si allega anche copia conforme agli originali.

Elenco Pubblicazioni redatte nel corso del SAL 2020

ENEA

1) Atrigna M.; Adinolfi, G.; Ciavarella R.; Graditi, G.; Merola R.; Ricca, A.; Valenti, M. (**2021**). A novel Tool for Hybrid AC/DC Grids Optimization and Reliability Assessment, 2021 IEEE International Conference on Environment and Electrical Engineering and 2021 IEEE Industrial and Commercial Power Systems Europe (EEEIC / I&CPS Europe), pp. 1-6, doi: 10.1109/EEEIC/ICPSEurope51590.2021.9584648.
2) Adinolfi G.; Ciavarella R.; Ricca A.; Merola A.; Valenti M.; Graditi, G. (**2021**). A reliability prediction model for power transformers, 2021 IEEE International Conference on Environment and Electrical Engineering and 2021 IEEE Industrial and Commercial Power Systems Europe (EEEIC / I&CPS Europe), pp. 1-4, doi: 10.1109/EEEIC/ICPSEurope51590.2021.9584596.
3) Sforza, G.; Adinolfi, G.; Atrigna, M.; Buonanno, A.; Ciavarella, R.; Merola, A.; Pascarella, F.; Ricca, A.; Valenti, M.; Graditi, G. (**2021**). PowerLab: a flexible experimental architecture for smart microgrid testing, 2021 IEEE International Conference on Environment and Electrical Engineering and 2021 IEEE Industrial and Commercial Power Systems Europe (EEEIC / I&CPS Europe), pp. 1-6, doi: 10.1109/EEEIC/ICPSEurope51590.2021.9584644.

Università di Palermo (UNIPA)

4) Bonì, A.; Favuzza, S.; Ippolito, M.G.; Massaro, F.; Modari, S.; Musca, R.; Porgi, V.; Zizzo, G. (**2021**). A Simulation Analysis for Assessing the Reliability of AC/DC Hybrid Microgrids – Part I: Underground Station and Car Parking, *2021 IEEE International Conference on Environment and Electrical Engineering and 2021 IEEE Industrial and Commercial Power Systems Europe (EEEIC / I&CPS Europe)*, pp. 1-6, doi: 10.1109/EEEIC/ICPSEurope51590.2021.9584826.
5) Bonì, A.; Favuzza, S.; Ippolito, M.G.; Massaro, F.; Modari, S.; Musca, R.; Porgi, V.; Zizzo, G. **(2021**). A Simulation Analysis for Assessing the Reliability of AC/DC Hybrid Microgrids – Part II: Port Area and Residential Area, *2021 IEEE International Conference on Environment and Electrical Engineering and 2021 IEEE Industrial and Commercial Power Systems Europe (EEEIC / I&CPS Europe),* pp. 1-6*, doi*: 10.1109/EEEIC/ICPSEurope51590.2021.9584607.

Università di Pisa (UNIPI)

6) Fioriti D., Lutzemberger G., and Poli D. (**2021**). Development of an Energy Management System for AC/DC hybrid networks: from abstract functional requirements to the flexible tool, *2021 IEEE International Conference on Environment and Electrical Engineering and 2021 IEEE Industrial and Commercial Power Systems Europe (EEEIC / I&CPS Europe),* pp. 1-6, doi: 10.1109/EEEIC/ICPSEurope51590.2021.9584645.

Università di Milano (POLIMI)

7) Navoni I.; Longo M. and Brenna M. (**2021**). Bidirectional Solid-State Circuit Breakers for DC Microgrid Applications" *2021 IEEE International Conference on Environment and Electrical Engineering and 2021 IEEE Industrial and Commercial Power Systems Europe (EEEIC / I&CPS Europe)*, 2021, pp. 1-6, doi: 10.1109/EEEIC/ICPSEurope51590.2021.9584802.

3.1 A novel Tool for Hybrid AC/DC Grids Optimization and Reliability Assessment

A novel Tool for Hybrid AC/DC Grids Optimization and Reliability Assessment

Mauro Atrigna
ENEA
Department of Energy Technologies and Renewable Sources
00196 Rome, Italy
mauro.atrigna@enea.it

Giovanna Adinolfi
ENEA
Department of Energy Technologies and Renewable Sources
00196 Rome, Italy
giovanna.adinolfi@enea.it

Roberto Ciavarella
ENEA
Department of Energy Technologies and Renewable Sources
00196 Rome, Italy
roberto.ciavarella@enea.it

Giorgio Graditi
ENEA
Department of Energy Technologies and Renewable Sources
00196 Rome, Italy
giorgio.graditi@enea.it

Angelo Merola
ENEA
Department of Energy Technologies and Renewable Sources
00196 Rome, Italy
angelo.merola@enea.it

Antonio Ricca
ENEA
Department of Energy Technologies and Renewable Sources
00196 Rome, Italy
antonio.ricca@enea.it

Maria Valenti
ENEA
Department of Energy Technologies and Renewable Sources
00196 Rome, Italy
maria.valenti@enea.it

***Abstract*—The growing interest towards the renewable energy sources remarks the relevance of smart grid exploiting in the electrical scenario. If in one hand smart grids introduces new perspective in the global energy management, on the other hand such innovative approach highlights the necessity to face with several issues related to the hybrid networks. Among them, the reliability of AC/DC hybrid grids is a crucial aspect for the effective development of hybrid smart grid. Studies on reliability of hybrid grids are present in the literature at component level, while the reliability related to the integration of smart grids in a traditional AC network is not exhaustively discussed. The present work proposes a Reliability Assessment Tool (RAT) aimed to the evaluation of specific hybrid grid configurations, as well as to manage contingency issues aimed to improve the safety and sustainability performances.**

Keywords—hybrid grids, microgrids, reliability assessment tool, optimization

I. INTRODUCTION

Microgrids (MG) are key factors for enabling a paradigm shift from large fossil fuel-fired power systems to localized and distributed generation. The chance to isolate MGs from the larger distribution grid makes power systems more flexible, resilient and competitive and allows the integration of higher share of volatile renewables [1]. Thus far, AC MGs have been the most used configuration, but AC-DC hybrid MGs are gaining interest due to the benefits provided by the DC MGs (no synchronization need, reducing number of DC-AC conversions, no reactive power, etc.). Therefore, evaluating the reliability of AC-DC hybrid MGs is essential, but also a challenge due to the relative novelty of the topic and the limited number of models currently available to evaluate the reliability of AC-DC hybrid MGs and their components [2], [3].

A microgrid is not characterized by a single technology, but it incorporates a wide number of generations, loads, interconnections between several devices and its control systems [4]. In a complex project, it is necessary to assure an appropriate generation sizing in order to satisfy steady state constrains, an appropriate conductors' sizing to assure the correct voltage levels, the validation of the controls supporting actions to manage, and the validation of the protections and the simulations of abnormal conditions [5]. A unified tool is not present among the commercial technical software, and the design of microgrid is only possible by using different tools: such approach is required because in the design phase several simulations characterized by different nature and different analytic base are employed. In addition, it is not usual that used software relies to different degree of readiness, while a wide number of simulations are necessary in the grid design phase. Therefore, despite a large number of tools are available for the different simulation scenarios [6], a lack of overall technology is still present for the comprehensive microgrid controls simulation devoted to the reliability assessment.

In this context, the project 2.7 "Models and tools to increase energy efficiency in the cycle electricity generation-transport- distribution"– aims to study, design and develop methodologies and tools for evaluating and improving the reliability of AC/DC distribution hybrid grids at Medium Voltage (MV) and Low Voltage (LV) levels. This goal will be achieved by designing and developing several research products:

- reliability assessment models for evaluating, in simulation environment, reliability indices for hybrid AC/DC (MV and LV) topologies, including enabling technologies for future energy scenarios;
- control actions improving the reliability of AC/DC hybrid MGs in both stationary and dynamic regimes;
- energy management logics for AC/DC hybrid MGs;
- power system protection logics and schemes for the reliability improvement.

This research was funded by the Research Fund for the Italian Electrical System under the Contract Agreement "Accordo di Programma 2019-2021 PTR_19_21_ENEA_PRG_10" between ENEA and the Ministry of Economic Development.

978-1-6654-3613-7/21/$31.00 ©2021 IEEE

All models are integrated and aggregated in a novel Reliability Assessment Tool (RAT) aiming to evaluate the reliability of specific grid configurations as well as to manage their contingency issues for improving the safety and suitability performances.

The tool is focused on AC/DC hybrid MGs at MV and LV voltage levels and considers operation issues by introducing controllers to solve them while improving reliability.

By integrating several methods for the reliability evaluation (at different levels) and management of grid criticalities, the RAT emerges an as useful tool in supporting AC/DC hybrid MGs development utilizing flexibility potential coming from renewables and emerging technologies such as storage systems, demand response and electric vehicles for contributing to the achievement of the 2030 and 2040 EU energy and climate objectives.

II. DESCRIPTION

A. Overview

The proposed tool offers methodologies to analyse and improve the reliability of AC/DC hybrid networks, both in medium voltage and low voltage. The core of the approach is focused on the evaluation, in the simulation environment, of the reliability of hybrid network setup in which crucial technologies for the ongoing energetic scenarios are included. In details, the proposed tool is developed according to a modular approach, thus enabling the evaluation of the reliability for specific network configurations, as well as the application of specific procedures aimed to the contingency management and to the system performances improvement in terms of safety and adequacy. In this sense, the proposed tool enables facing management issues for the integration of innovative MV/LV DC grids in the existing AC grids, thus assuring an overall reliability improvement for the network. The proposed approach arouses further interest in a scenario in which the presence of distributed generation via renewables and electrical vehicles recharge stations is more significant.

The evaluation of the reliability of the network, and its components, is based on peculiar parameters for the network items, as well as on the operative data: this approach allows to carry on comparative reliability analyses of different topologic solutions, thus enabling the definition of novel paradigms in the context of interconnected hybrid network. The comparison between reliability indexes of the different configurations, in a conceptual point of view, defines a ranking of the proposed topologies, providing relevant information for the future development of electrical hybrid grids and for the spread of innovative energetic scenarios, thus resulting in noticeable positive drawbacks for the electrical system. In fact, the possibility of identifying of reliable configurations enables selecting the most performant solutions in terms of electrical services continuity.

B. Configurations

From a practical point of view, the user can select 3 different analysis typologies:

Basic configurations: It is possible to calculate the reliability of a (hybrid) grid through selected reliability indexes, and to evaluate the interruption costs based on the referenced time interval. The tool will automatically simulate contingency events for the selected grid architecture, applying the reliability models for the involved grid components. Thus, the overall grid configuration reliability will be evaluated, and in addition the contingency solution actions will be simulated.

Advanced configurations on specific logics: actions related to 3 specific logics are applicable by the tool: protections, controls and energy management. By selecting a specific logic, the tool will enable a different configuration (on the basis of the selected logics, e.g., considering supplementary protection devices if "protection" is selected, or by managing controllable loads if "controls" is selected), thus evaluating the reliability degree for the new configuration. The comparison between the basic and the advanced configurations will provide the effectiveness of the proposed actions, in terms of evaluation of system reliability improvement.

Advanced configuration on multiple logics: Such modality allows to simultaneously test two or more actions/logics. Also in this case, the user can understand the effectiveness of the proposed action in terms of system reliability improvement. In addition, such configuration will also highlight the impact related to the interference between the different control stages, thus providing relevant information about the advantages of applying one or more control actions to the innovative AC/DC hybrid networks.

C. Structure

The proposed tool allows to operate on pre-loaded (workbench) or user-defined networks configurations for reliability analysis. The workbench networks focus on typical grid representing a city area and a port area, simulating realistic configurations. For each workbench network five scenarios could be selected, corresponding to the Italian electrical distribution system referred to the year 2020, and to other 4 forecasted scenarios corresponding to the years 2030 and 2040, assuming an increasing of renewable energy resources exploitation in a centralized or in a distributed context.

Starting from a load flow analysis, it is possible to select the analysis target (economic or reliability), it is possible to evaluate reliability indexes or interruption costs. Moreover, the tool is able to simulate reliability models for each grid component, allowing the overall network reliability evaluation in the selected grid configuration and simulating solution actions. In particular, it is possible to simulate each action for protection device, control and energy management, thus validating the effectiveness of the proposed actions in terms of system reliability improvement, as well as renewable resource exploiting. The outcoming results will be accurately documented, describing the operating conditions for each action and/or multiple control logics, aimed to the reliability performances for the selected grid.

The Reliability Assessment Tool is developed in Python language, offering to the users a user-friendly interface from which it is possible to access to all the functionalities. It integrates the possibility to be interfaced with two of the most diffused software for the grid analysis: DIgSilent PowerFactory® and Neplan®. In both cases, the user can charge in the tool custom grids designed with the former mentioned software.

For the integration with PowerFactory, the tool requires that the simulation software should be installed on the client PC in order to exploit the interface between the tool and the

software; the tool will communicate with the PowerFactory in background, thus the software interface should be off.

The integration with Neplan is based on WebServices: such feature does not require that the software should be installed on the client PC, since it exploits remote licences with the software house.

All the RAT functionalities refer to the analysis modes embedded in the dedicated software (LoadFlow, EMS, RMS, Reliability Analysis, etc.), or to dedicated Python scripts devoted to custom analysis, protection devices simulation and grid controls for performances optimization.

III. TOOL FUNCTIONALITIES

A. *First stage: analysis selection*

In the proposed tool, user can select 3 different analysis criterions to be considered for the operations on the grid under investigation. In particular, the choice is addressed between:

- Grid electrical protection, in which it is possible to define the optimal protection suitable to the grid under investigation, or a technical/economic analysis for a protection system based on different types (e.g., electromechanical, electronic, etc.).
- Reliability evaluation for the grid elements, through models based on experimental data or design standard references.
- Grid reliability optimization through the striking of technical or economic goals, by describing the existing system operation in terms of storage capacity, electrical power feed duty, operation time, etc. This stage includes advanced control strategies for evaluating the optimal set of resources (i.e., the grid configuration) to avoid grid issues (e.g., congestion) while improving grid reliability.

After defined the desired function, the user in a first stage (Fig.1) can select the simulation functionality, the performances indicator, and the operating scenario.

B. *Second stage: Network characterization*

In a second stage (Fig. 2), the user can select a grid in which an equivalent methodology is applicable: the equivalent methodology allows simplifying some grid sub-parts, assuring the interaction and flexibility features for the distributed resources; alternatively, the user can use a custom model of an electrical grid, according to the design constrains necessary for a full compatibility with the tool.

More in the detail, the user can choose to import in the tool a custom network model (generated with DIgSilent PowerFactory or Neplan based on the selected analysis type) or can select one of the proposed benchmark networks. In the latter case, the user can choose to load a specific scenario: in particular, the scenario 2020 is representative of a nowadays electrical situation in Italy. Scenarios 2030 and 2040 represents a forecasted modification of energy consumption and renewable generation penetration. In particular, for both years, an enlargement of renewable production plants and storage systems was simulated, moreover it was simulated a case in which renewable penetration is more relevant in a centralized production (CEN), and a case in which the renewable penetration is more relevant in a distributed production (DEC). Therefore 5 scenarios were selectable for each benchmark networks: 2020; 2030-CEN; 2030-DEC; 2040-CEN; 2040-DEC.

After selected the network model to be investigated, the tool will ask to the user to provide parameters and time series based on the pre-defined analysis in order to totally characterize the grid under investigation. In particular, PVs and wind power generators size, energy storage capacity, lines length, conversion unit size, etc. could be totally customized on the basis of specific requirements of the tool's user. In addition, time series for the loads' duty, or for the generation plants productivity could be selected among a list of pre-set curves; moreover, custom profiles could be imported by users for each device, or for groups of them. At the end of this stage, the network is totally configured, and the scenario is defined, thus the network is ready for the analysis stage. It is worth noting that the network configuration and the defined scenario could be exported by the user, thus allowing a fast reconfiguration in future analyses.

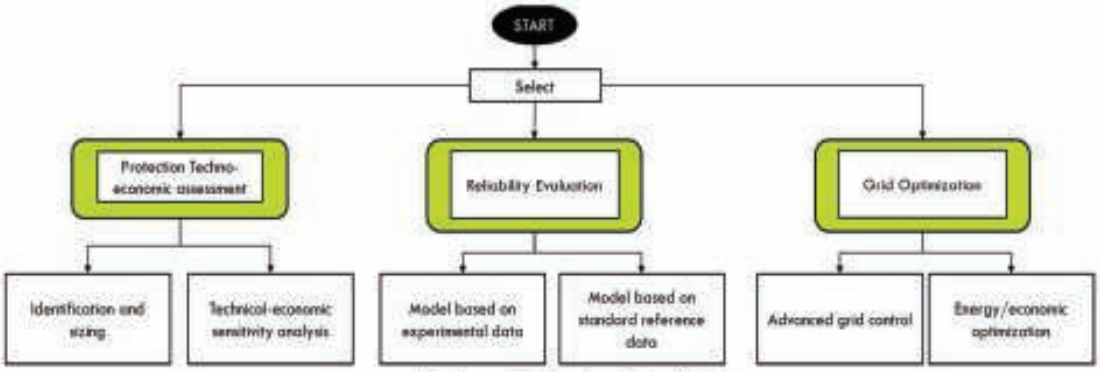

Fig. 1. Tool functionalities – first stage

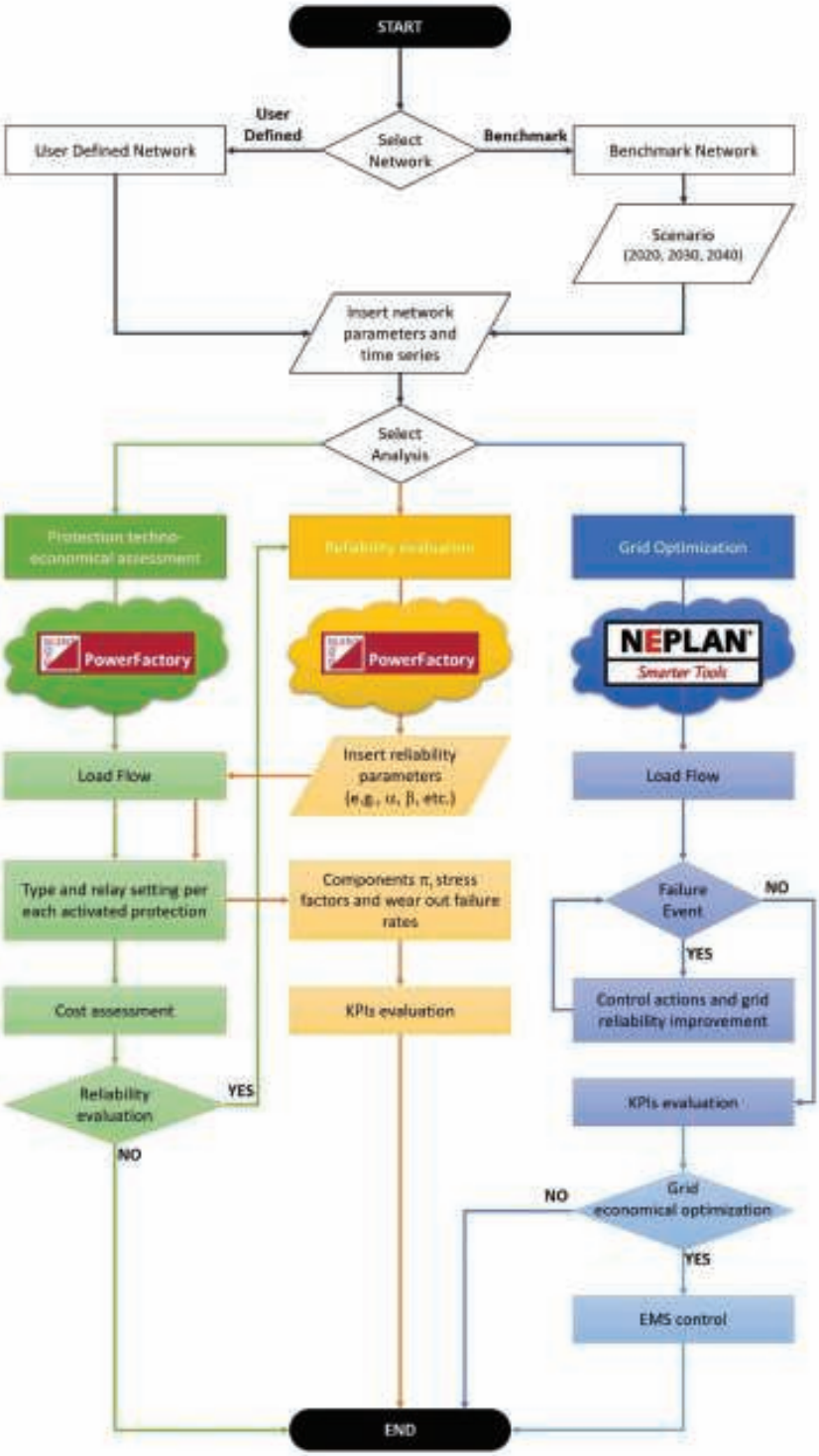

Fig. 2. Optimization and reliability assessment tool conceptual scheme

C. Third stage: simulation and results

Finally, in the third stage the tool will carry on the simulation, responding with the analysis results. The methodologies implemented in the proposed tool, described through a dedicated compilation form in the early stages, allow to user the selection of the most suitable solution on the basis of the identified operating function to be employed for the investigated distribution grid and scenario.

The description and grid composition stages are designed to guide users in order to select the most appropriate control or protection, on the basis of the required goal for the grid under investigation. The simulation functionalities are selectable among a list related to the use cases. KPI and operative scenarios are enabled according to the admittible combinations, on the basis of previously selected study cases; each study case requires a specific functionality simulation.

1) Protection and techno-economical assessment

In the case of the protection and techno-economical assessment, the tool in carry out a load flow analysis through the PowerFactory software, that provides a full frame of the grid in the selected scenario. Once defined the grid model status, the tool will run a custom routine aimed to define the type, the number and the relay setting for the activated protection. Finally, the tool will perform a cost assessment for the proposed solution, in order to provide to the used a clear overview of the protection impact on the grid under investigation.

At the end of the analysis, the user can choice to either perform a reliability analysis of the grid, or if the analysis is terminated. In the latter case, a report file was generated in which the protection configuration and the economic analysis are summarized. In the other case, the Reliability Evaluation routine will be performed.

2) Reliability evaluation

In the reliability evaluation, the RAT tool will perform a detailed analysis of the reliability of each component of the grid under investigation, as well as of the network as a whole. Based on the reliability prediction methods reported on the MIL-HDBK-217F [7] and FIDES 2019 [8] guides, the tool invites the user to provide a series of reliability parameters for each element in the network, on the basis of the related operating conditions. Alternatively, the user can select default parameters for the components, accepting a reduced accuracy of the downstream evaluations.

Once characterized the network under the reliability point of view, the tool will perform a LoadFlow analysis through the PowerFactory software. In addition, the tool will identify all the protections in the network, that will be considered in the reliability analysis.

Once defined the operating conditions of the grid, the tool will carry out the failure rate of each component, through the evaluation of their stress factors at the selected operation status. The approach for the evaluation of the failure rate of the components though the calculation of stress factors is reported elsewhere [9]. Finally, the failure rate of the global network, or of branches of it (to be selected by the user through a dedicated interface) will be carried out, and KPIs parameters (mostly composed by reliability indexes) will be stored in an output file.

3) Grid optimization

The grid optimization functionality aims to define a grid analysis and a network reconfiguration in order to counter failure events, thus improving the global reliability, or to achieve an economical optimization.

The failure events should be embedded in the grid model file (to be generated through Neplan software). If no failure events are defined in the file, the tool will prompt to the user a dedicated interface for define the position and the nature of the failure event. In the case the user will skip the failure event definition, the sub-routine inherent to the failure event management will be skipped.

At the beginning of the routine, the tool will perform a LoadFlow analysis through the Neplan software, to define the operating conditions of the model. Then the tool checks whether any failure event is occurring in the network (of course, in the first run of the software, the failure event is defined by the user). If a failure event is detected, the software will start a sub-routine in which the control actions operate to solve the grid failure and then to improve the network reliability. After each control actions stage, the RAT tool will repeat the LoadFlow analysis in order to check whether other failure events are present in the network under investigation (maybe generated, in a different section of the grid, by the former control actions). The control actions will be repeated until any failure event is present in the network model; once solved any failure event issue, the results of the control actions and the reliability analysis results will be reported in a file.

Once concluded the failure event management, the user can decide to operate an economical optimization of the grid under investigation, in which renewable energy resources, and the relative energy storage systems, will be reconfigured in order to maximize the RES exploiting. The EMS control will operate on a defined time range, according to the time series selected by the users in the early stage of the tool. Dedicated datasheet and time-diagrams will be provided at the end of the EMS control in order to show the control actions, and to highlight the economical (or technical) advantages generated by the tool.

IV. CONCLUSIONS

This paper presents a brief description of the methodology devised within the project 2.7 "Models and tools to increase energy efficiency in the cycle electricity generation-transport-distribution", aimed at facilitating and improving power system reliability and operation, with special focus on high-RES penetration, a challenge for the future 2030+ power networks. The methodology described in this paper will be transformed into a Python-based toolbox interfacing with DIgSILENT PowerFactory and Neplan in the simulation phase in stages 2 and 3.

The three main stages of the tool allow the grid optimization from a techno-economical point of view, the protection sizing and choosing and the reliability evaluation for hybrid AC/DC grids.

The proposed tool integrates assessment and optimization features. The user can evaluate the reliability at system and component levels, and improve it by acting on the grid configuration (e.g., resources redistribution, islanding of specific grid areas, etc.) or by operating each component according to conditions aimed at improving its reliability (e.g., by reducing over-temperature in operation). Furthermore, two

additional features allow to identify and size the protection devices integrated into the grid, and to perform the energy/economic optimization of the system for maximizing the renewable exploitation respectively.

ACKNOWLEDGEMENT

The authors would like to acknowledge the Research Fund for the Italian Electrical System for funding this work through the project "Accordo di Programma 2019–2021 PTR_19_21_ENEA_PRG_10" between ENEA and the Ministry of Economic Development.

REFERENCES

[1] D. E. Olivares, C. A. Canizares, and M. Kazerani, "A Centralized Energy Management System for Isolated Microgrids," IEEE Trans. Smart Grid, vol. 5, no. 4, pp. 1864–1875, Jul. 2014.

[2] A. Naderipour, H. Saboori, H. Mehrjerdi, S. Jadid, and Z. Abdul-Malek, "Sustainable and reliable hybrid AC/DC microgrid planning considering technology choice of equipment," Sustain. Energy, Grids Networks, vol. 23, p. 100386, 2020.

[3] A. Abdelsamad and D. Lubkeman, "Reliability Analysis for a Hybrid Microgrid based on Chronological Monte Carlo Simulation with Markov Switching Modeling," in 2019 IEEE Power & Energy Society Innovative Smart Grid Technologies Conference (ISGT), 2019, pp. 1–5.

[4] M. Jayachandran and G. Ravi, "Design and Optimization of Hybrid Micro-Grid System," Energy Procedia, vol. 117, pp. 95–103, June 2017.

[5] M. Kharrich et al., "Optimal Design of an Isolated Hybrid Microgrid for Enhanced Deployment of Renewable Energy Sources in Saudi Arabia," Sustainability, vol. 13, no. 9, p. 4708, Apr. 2021.

[6] O. K. P. Mokoka and K. O. Awodele, "Reliability Evaluation of distribution networks using NEPLAN & DIgSILENT Powerfactory," in 2013 Africon, 2013, pp. 1–5.

[7] U.S.A. Department of Defense, MIL-HDBK-217F - Military Handbook - Reliability prediction of electronic equipment, F. Washington, D.C., 1990.

[8] FIDES Group, "FIDES guide 2009 - Reliability Methodology for Electronic Systems," 2010.

[9] G. Adinolfi, R. Ciavarella, G. Graditi, A. Ricca, and M. Valenti, "A Planning Tool for Reliability Assessment of Overhead Distribution Lines in Hybrid AC/DC Grids", Sustainability, vol. 13, no. 11, p. 6099, May 2021.

3.2 A reliability prediction model for power transformers

A reliability prediction model for power transformers

Giovanna Adinolfi
Dept. of Energy Technologies
ENEA, Research Centre
Piazzale E. Fermi, 1
80055, Portici, Napoli, Italy
giovanna.adinolfi@enea.it

Roberto Ciavarella
Dept. of Energy Technologies
ENEA, Research Centre
Piazzale E. Fermi, 1
80055, Portici, Napoli, Italy
roberto.ciavarella@enea.it

Antonio Ricca
Dept. of Energy Technologies
ENEA, Research Centre
Piazzale E. Fermi, 1
80055, Portici, Napoli, Italy
antonio.ricca@enea.it

Angelo Merola
Dept. of Energy Technologies
ENEA, Research Centre
Piazzale E. Fermi, 1
80055, Portici, Napoli, Italy
angelo.merola@enea.it

Maria Valenti
Dept. of Energy Technologies
ENEA, Research Centre
Piazzale E. Fermi, 1
80055, Portici, Napoli, Italy
maria.valenti@enea.it

Giorgio Graditi
Dept. of Energy Technologies
ENEA, Research Centre
Via Anguillarese, 301
00123, Roma, Italy
giorgio.graditi@enea.it

***Abstract*— Power systems reliability assessment represents a complex task due to large number of systems and subsystems and for the significant number of different stresses affecting on individual components. Different models, methods and metrics can be used for electric and electronic systems in specific applications. The aim of this paper consists in the development of a reliability prediction models for power transformers in hybrid AC/DC grids. Future energy scenario with bidirectional power flows could stress transformers components. The propose approach intends to evaluate thermo-mechanical, environment and quality stress factors for each transformer subsystem with particular attention to ageing phenomena. The overall transformer reliability performances are calculated in real operating conditions characterizing 2030 scenarios.**

Keywords—power transformers, thermo-mechanical stress, style, stress factors, failure rate

I. INTRODUCTION

Traditional power systems were organized according to unidirectional power flows from generators to users. Nowadays the energy paradigm is changing toward bidirectional models including renewables sources [1] and distribute storage systems.

In this context, power systems operating conditions are modified and usually grids systems and devices are subject to stressful conditions that affecting their performance in the short and long term.

This paper focuses the attention on power transformer in hybrid AC/DC grids characterized by Low Voltage and Medium Voltage DC microgrids able to inject power into the main AC grid. In this specific application, a huge number of interface converters must be employed with bidirectional, overloading and harmonics criticalities impacting grid devices performance.

The transformer represents a crucial element for the correct functionality of the electrical system. The choice of a specific type of transformer depends on many factors, among which the most significant are environmental conditions, place of installation, fire hazard, thermal behaviour, pollution, maintenance, type of users to be powered. The most used types of transformers are transformers with liquid dielectric (mineral oil or silicone oil) and dry transformers with resin insulation.

Failure of the transformer can not only affect the continuity of service of various users, but can also cause extensive damage (oil leakage, explosions, fires). Therefore, the definition of a model characterizing its reliability performance in recent real operating contexts represents a crucial task [2-3].

In literature, a reliability model for Oil Natural Air Natural (ONAN) transformers is proposed in [4] according to a Markov process representation. Transformer performances by Markovian approaches are also analysed in [5-7], while in [8] a reliability model is proposed and developed based on field data. In this paper, an alternative approach is implemented by considering transformer main subsystems and analysing thermo-mechanical, environment and quality stress factors, also including ageing phenomena impact, affecting the reliability. Based on this approach, a reliability prediction model for power transformers is developed.

The paper is organized as follows: the first section describes the power transfomers reliability prediction model and all functions, indexes and hypothesis considered for its development; in the second section, the model is applied to a case study constructed by supposing a MV/LV transformer connected to a 2030 grid. Finally, the main results are summarized in the conclusions.

II. POWER TRANSFOMERS RELIABILTIY MODEL

The transformer functioning mode is modelled by means of the corresponding equivalent circuit whose parameters are calculated starting from manufacture provided data.

Climatic timeseries (ambient temperature data, relative humidity, irradiation, wind speed of the sites installation) and grid generation, loads and storage equipment profiles are necessary input to study the transformer operating mode in real conditions (Fig. 1).

This research was funded by the Research Fund for the Italian Electrical System under the Contract Agreement "Accordo di Programma 2019–2021 PTR_19_21_ENEA_PRG_10" between ENEA and the Ministry of Economic Development.

978-1-6654-3613-7/21/$31.00 ©2021 IEEE

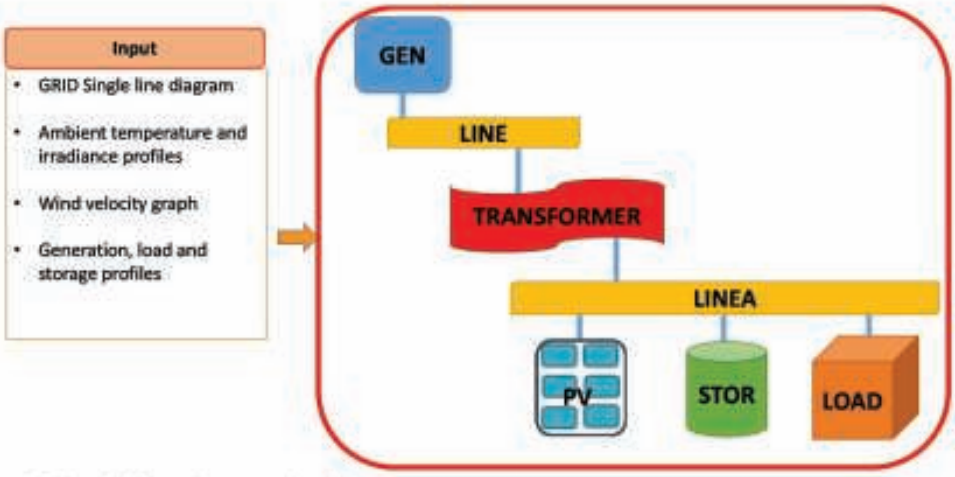

Fig. 1. Grid Schematic representation and inputs

In detail, the main subsystems of a power transformer consist of the windings, the core and the oil tank in ONAN transformers. For the purposes of assessing reliability, the transformer is considered as a system consisting of the connection between these three subsystems.

This is a series-type logical connection in the sense that it is enough for one of the three subsystems to be in fault conditions to affect the functionality of the entire transformer. The failure rate will therefore be determined by the following formula:

$$\lambda_{TRAN}(t) = \lambda_{windings}(t) + \lambda_{core}(t) + \lambda_{dielectric}(t) \quad (1)$$

where:

- $\lambda_{windings}$ = windings failure rate;
- λ_{core} = core failure rate;
- $\lambda_{dielectric}$ = dielectric liquid failure rate;

In the proposed model each failure rate is calculated according to Eq.2 [9]:

$$\lambda(t) = \lambda_{invecchiamento}(t) \cdot (\pi_S + \pi_E + \pi_Q + \ldots \pi_Y) \quad (2)$$

where:

- π_S is the thermos-mechanical stress factor;
- π_E is the environment factor;
- π_Q is the quality factor;
- $\lambda_{invecchiamento}$ is the failure rate due to aging phenomena

In this paragraph authors proceed with the assessment of the stress factors affecting each subsystem of the transformer.
With reference to the windings, the thermo-mechanical phenomena affecting both the copper conductors and the insulation are considered.

Input times series and manufacturer rating data allow the calculation of the resistances of the windings on the primary and secondary of the transformer in the different considered operating conditions.
Then overtemperature and, therefore, the operating temperature for each operating condition is calculated. The innovative aspect is represented by the overtemperature estimations obtained considering not only transformer copper losses but also installation operating conditions in terms of temperature and irradiance. The identification of the maximum operating temperature among calculated ones and the subsequent introduction of this value in the Norris-Landzberg (Eq.3) model will allow to quantify the thermos-mechanical stress factor for transformer windings.

$$\pi_S = \left(\frac{12 \cdot N_{annual\_cy}}{t_{annual}}\right) \cdot \left(\frac{\Delta T_{cycling}}{20}\right)^{ma} \cdot \exp\left[1414 \cdot \left(\frac{1}{313} - \frac{1}{T_{max\_cy}}\right)\right] \quad (3)$$

where:

- T_{amb} = Ambient Temperature (K)
- N_{annual_cy} = Cycles in a year (cycles)
- t_{annual} = Time over a year (hours)
- $\Delta T_{cycling}$ = Temperature range in a cycle (K)
- T_{max_cy} = Max temperature in a cycle (K)

In the implemented model winding conductor thermal data are used to calculate insulating layer temperature and the consequent π_S factor.
In a similar manner thermo-mechanical stresses are evaluated for transformer core and dielectric liquid.

The environmental stress π_E is determined by the environmental stresses affecting the system of interest. Similar to Military Handbook 217F. The types of

environment considered in the specific context of electricity grids are:

- Ground, G: a non-mobile environment, characterized by uncontrolled temperature and humidity;
- Ground, Benign GB: it represents a non-mobile environment, easily accessible for maintenance, characterized by controlled temperature and humidity.
- Ground, Fixed GF: it represents a moderately controlled environment with an adequate cooling system and possible installation in unheated buildings.
- Naval, Unsheltered NU: it represents the environment in which surface naval equipment is placed, unprotected, exposed to weather conditions and equipment immersed in salt water;
- Naval N: it represents an underwater environment.

In the reliability model, the π_Q factor provides an evaluation of the quality level of a system/device that depends on how the production process takes place. In fact, the products can be manufactured in a qualitatively different manner in accordance with specifications and standards for use in military or commercial applications.

The wear of a system due to aging phenomena is considered in the reliability model of each element by means of the failure rate $\lambda_{wear\,out}$. It is determined on the basis of the results of studies on the subject which have shown that the experimental data fit the Weibull distribution with scale factor α and the form factor β, as reported in Eq. 4.

$$F(t,\alpha,\beta) = 1 - e^{-\left(\frac{t}{\alpha}\right)^{\beta}} \qquad t > 0 \tag{4}$$

The proposed reliability model therefore allows to represent each system or subsystem by means of the failure rate λ determined by the joint action of the stresses π_i (thermo-mechanical, environmental, etc.) considered and by the deterioration due to aging of the component and / or system of interest, as schematically reported in the following Eq. 5.

$$\lambda = \lambda_{wear\_out} \cdot \sum_i \pi_i \cdot \frac{failures}{10^6\ hours} \tag{5}$$

where π_i is the i-th stress factor.

III. A CASE STUDY

A case study represented by a MV/LV transformer connected to a 2030 grid is analysed by applying the described prediction model.

The studied transformer is affected by two thermal cycle/day with 90°C and 30°C maximum and minimum cycle temperature values respectively.

Furthermore, it is subjected to ageing phenomena modelled by the above reported Weibull distribution characterized by a scale factor of 5200000 hours and a shape factor of 2.

The application of the proposed model provides the evaluation of affecting stressed (by π_i factors values) and reliability indices.

In detail, the transformer is installed in a non-mobile environment, characterized by uncontrolled temperature and humidity. It is manufactured with system and subsystem quality level according to IEC 60076-11.

In those conditions, the following π_i factors and failure rates are obtained.

$$\pi_S = 1.626 \tag{6}$$

$$\pi_E = 6 \tag{7}$$

$$\pi_Q = 1 \tag{8}$$

$$\lambda_{wear\_out} = 3.2396 \cdot 10^{-7}\,\frac{failure}{hours} \tag{9}$$

$$\lambda_{TRAN} = 2.7934 \cdot 10^{-6}\,\frac{failure}{hours} \tag{10}$$

The calculated failure rate demonstrates the system reliability level due to achieved technology maturity.

This case study has also been analyzed to validate the proposed reliability prediction model which can be applied to different power systems components and to different energy paradigms. The identification of reliability criticalities in grids and micro-grids could contribute to design, optimize and control the power systems devices in order to assure service continuity and overstressing conditions avoidance.

CONCLUSIONS

This paper proposes a reliability prediction model for power transformers by considering windings, core and dielectric liquid subsystems and estimating related affecting stress factors.

In detail, thermo-mechanical, environment and quality factors are calculated to quantitatively estimate the whole converter failure rate. Furthermore, ageing phenomena are taken into account to an accurate reliability evaluation. A transformer case study is analysed to evaluate reliability indices and to validate the proposed prediction model.

Without loss of generality, the reported reliability prediction model can be applied to different power systems components.

ACKNOWLEDGEMENT

The authors would like to acknowledge the Research Fund for the Italian Electrical System for funding this work through the project "Accordo di Programma 2019–2021 PTR_19_21_ENEA_PRG_10" between ENEA and the Ministry of Economic Development.

REFERENCES

[1] G. Graditi, G. Adinolfi , "Temperature influence on Photovoltaic Power Optimizer Components Reliability", International Symposium

on Power Electronics, Electrical Drives, Automation and Motion, pp. 1113-1118, 2012.

[2] G. Graditi, G. Adinolfi, A. Pontecorvo, "RIAC 217 Plus reliability prediction model in photovoltaic systems", International Conference on Clean Electrical Power, pp. 11 – 13, 2013.

[3] G. Graditi, G. Adinolfi, A. Del Giudice, "Experimental performances of a DMPPT multi-topology converter", International Conference on Renewable Energy Research and Applications, pp. 1005-1009, 2015.

[4] M. Sefidgaran, M. Mirzaie, and A. Ebrahimzadeh, "Reliability Model of Power Transformer with ONAN Cooling," Elsevier International Journal of Electrical Power & Energy Systems, vol. 35, pp. 1–20, April 2012.

[5] R. Billinton, M. Fotuhi-Firuzabad and alii, ., "Determination of theoptimum routine test and self checking intervals in protective relaying using a reliability model", IEEE Trans. on Power Systems, vol. 17, pp. 663-669, 2002.

[6] H. Seyedi, M. Fotuhi, and M. Sanaye-Pasand, "An extended Markov model to determine the reliability of protective system", Power India Conference, IEEE, 2006.

[7] F.Aminifar, M. F. Firuzabad, and R. Billinton, "Extended reliability model of a unified power flow controller", Generation, Transmission and Distribution, IET, vol. 1, , pp. 896-903, 2007.

[8] M. Chafai, L. Refoufiand alii, "Large power transformer reliability modeling", International Journal of System Assurance Engineering and Management, vol. 7, pp. 9–17, 2016.

[9] G. Adinolfi, R. Ciavarella, G. Graditi, A. Ricca, and M. Valenti, "A Planning Tool for Reliability Assessment of Overhead Distribution Lines in Hybrid AC/DC Grids," Sustainability, vol. 13, no. 11, p. 6099, May 2021.

3.3 PowerLab: a flexible experimental architecture for smart microgrid testing

PowerLab: a flexible experimental architecture for smart microgrid testing

Gianluca Sforza
Dept. of Energy Technologies and Renewable Energy Sources
ENEA
Rome, Italy
gianluca.sforza@enea.it

Giovanna Adinolfi
Dept. of Energy Technologies and Renewable Energy Sources
ENEA
Rome, Italy
giovanna.adinolfi@enea.it

Mauro Atrigna
Dept. of Energy Technologies and Renewable Energy Sources
ENEA
Rome, Italy
mauro.atrigna@enea.it

Amedeo Buonanno
Dept. of Energy Technologies and Renewable Energy Sources
ENEA
Rome, Italy
amedeo.buonanno@enea.it

Roberto Ciavarella
Dept. of Energy Technologies and Renewable Energy Sources
ENEA
Rome, Italy
roberto.ciavarella@enea.it

Angelo Merola
Dept. of Energy Technologies and Renewable Energy Sources
ENEA
Rome, Italy
angelo.merola@enea.it

Francesco Pascarella
Dept. of Energy Technologies and Renewable Energy Sources
ENEA
Rome, Italy
francesco.pascarella@enea.it

Antonio Ricca
Dept. of Energy Technologies and Renewable Energy Sources
ENEA
Rome, Italy
antonio.ricca@enea.it

Maria Valenti
Dept. of Energy Technologies and Renewable Energy Sources
ENEA
Rome, Italy
maria.valenti@enea.it

Giorgio Graditi
Dept. of Energy Technologies and Renewable Energy Sources
ENEA
Rome, Italy
giorgio.graditi@enea.it

***Abstract*—Interest in microgrids is advancing as they contribute to local energy management while preserving the main grid operation. However, their introduction poses problems of reliability, particularly when renewable sources are present. Therefore, devices and management systems need preliminary tests in lab facilities using emulators before their deployment on the field. This paper presents an architecture designed to help researchers test the envisioned management algorithms and control techniques on a lab-scale microgrid facility. On that base, a prototype control system was implemented to assess the operation in close to real conditions of an advanced control logic aiming at avoiding congestion issues. The physical architecture of the microgrid was easily adapted to the purpose. Results show that the microgrid effectively acted as expected, following the commands dispatched by the control system.**

This research was funded by the Research Fund for the Italian Electrical System under the Contract Agreement "Accordo di Programma 2019-2021 PTR_19_21_ENEA_PRG_10" between ENEA and the Ministry of Economic Development.

978-1-6654-3613-7/21/$31.00 ©2021 IEEE

***Index Terms*—smart microgrid, renewables, energy emulators, advanced control**

I. INTRODUCTION

A large electrification across all energy sectors is the key to achieve decarbonisation targets by 2050, but poses risks for the security and reliability of power systems [1]. The integration of microgrids (MGs) allows the gain of the advantages of electrification, while preserving correct working conditions of the overall network. Cooperation mechanisms between a variety of internal resources, as well as control-communication mechanisms towards the distribution grid, enable proper management of the MGs [2], [3]. In this scenario, lab-based experimental grids are essential for testing devices and smart management logics from the development to the prototypal stage. PowerLab is an experimental MG installed at ENEA Research Centre of Portici, based on a reconfigurable physical architecture and on a software management system that is scalable and open to embed new equipment. PowerLab MG can work in "island mode" or "connected" with the main grid.

Furthermore, it includes DC (range 40 V – 1000 V) and AC (range up to 300 V) levels; the MG can also be operated in "hybrid AC/DC mode". Testing larger systems on a lab-scale facility involves economic and space problems, which can be tackled with approaches combining the most significant methods for testing — real-time simulations, hardware in the loop (HIL) and emulation [4]. To enable the analysis of the behaviour of this MG within a distribution grid, an HIL system [5] is connected to the physical architecture of PowerLab.

Therefore, a combined approach using HIL simulation and hardware emulation can be adopted to study extended grids (e.g., distribution grids) including small size MGs. Here, the MG can be operated through PowerLab and interconnected — as a single technology — to the extended grids simulated with HIL. The designed MG can be used as testbed for diverse studies, including reliability and stability of a MG, control under particular operative conditions, communications, systems of multiple MGs, as well as feasibility studies. In particular, this architecture was designed with the purpose of simulating realistic setups and experimenting on energy management and other strategies relating to the MG's operation. Moreover, the time series formed by the stored measurements can be used in machine learning tasks, such as to increase the amount of data for training or to validate load forecasting methods [6]. While the software components required by this architecture are under development, a control system prototype was implemented, to test a possible use of the PowerLab MG related to an ancillary service and the reliability improvement of MG lines [7].

The paper is structured as follows. Section II describes the physical architecture of the microgrid. Section III describes the communication architecture designed. Section IV presents a case study tested on a prototype architecture. Section V summarises the main conclusions and the future work.

II. Physical architecture

The microgrid is currently operating as depicted in Fig. 1. It is composed of several units described below.

- A three-phase 30 kVA grid emulator with generative and regenerative capabilities. In generative mode (source) it operates using single or three phase output in AC or AC+DC mode, with pre- or user-defined voltage waveform;
- Three mono-phase 5 kVA grid emulators, with the same properties of output voltage waveform configuration;
- Three solar array simulators having a maximum power of 4.25 kW, in which the user can define the environmental parameters of solar irradiance and temperature to test conditions of shadowed and dirty photovoltaic arrays;
- A modular solar array simulator having a maximum power of 1.2 kW, composed of two internal modules that can operate in series or in parallel;
- A group of programmable DC power supplies that provide adequate power both to the DC-DC converters and to the inverters, including bipolar 4-quadrant and bidirectional regenerative power supplies; these DC power supplies allow the emulation of several distributed resources (e.g., electric vehicles - EV, storage systems, etc.);
- A group of programmable electronic loads, including a linear DC load that dissipates a maximum power of 0.8 kW and allows low-voltage operation;
- Three AC/DC loads providing parallel and 3-phase control, which dissipate a maximum power of 5.4 kVA and allow the simulation of a broad range of consumptions;
- A 15 kW non-linear AC/DC regenerative load that produces significant energy savings in cyclic testing;
- A photovoltaic experimental plant with a rated power of 1.2 kW, for testing in real outdoor conditions;
- A 50 kW Power Energy Interface;
- A 4.8 kWh Li-Ion battery system;
- A 300 Wh supercapacitor system;
- A device for real-time hardware-in-the-loop (HIL) simulation of the electric grid.

III. Communication architecture

The main variables to control in a microgrid are voltage, frequency, active and reactive power [8]. To accomplish this task, a hierarchical architecture was designed based on three layers (Fig. 2):

- The upper layer, that consists of the management services;
- The middle layer, to supervise and control all the instruments and meters (acting as a SCADA system);
- The bottom layer, with the local controllers of the instruments of emulation and the meters.

Hierarchical models [9] are adopted by several microgrid control systems in research labs [10]–[17]. Such an architecture can be operated in centralised or decentralised mode [9], depending on the functions assigned to the local controllers. Its flexible concept admits the integration of different communication protocols. In the following, the functionalities of each layer are detailed.

A. Middle layer

This layer accomplishes core tasks in the microgrid. The availability of two control centres is intended to lighten the workload of this layer. The control centre component coordinates the control actions over the instruments, manually given from the operator through the command services component, or sent by an energy management algorithm, and it routes the commands to the controllers of the instruments. It archives:

- The state of the instruments;
- Measurements locally generated by the instruments;
- All the events happened during its operation, e.g., control and measure events.

The measurements monitor centre component aggregates data produced by the meters located in strategic points of the whole network. Normally the meters are always active. This component receives manual configurations or it can be preset to work autonomously. Also, it supervises the status of the meters. It archives:

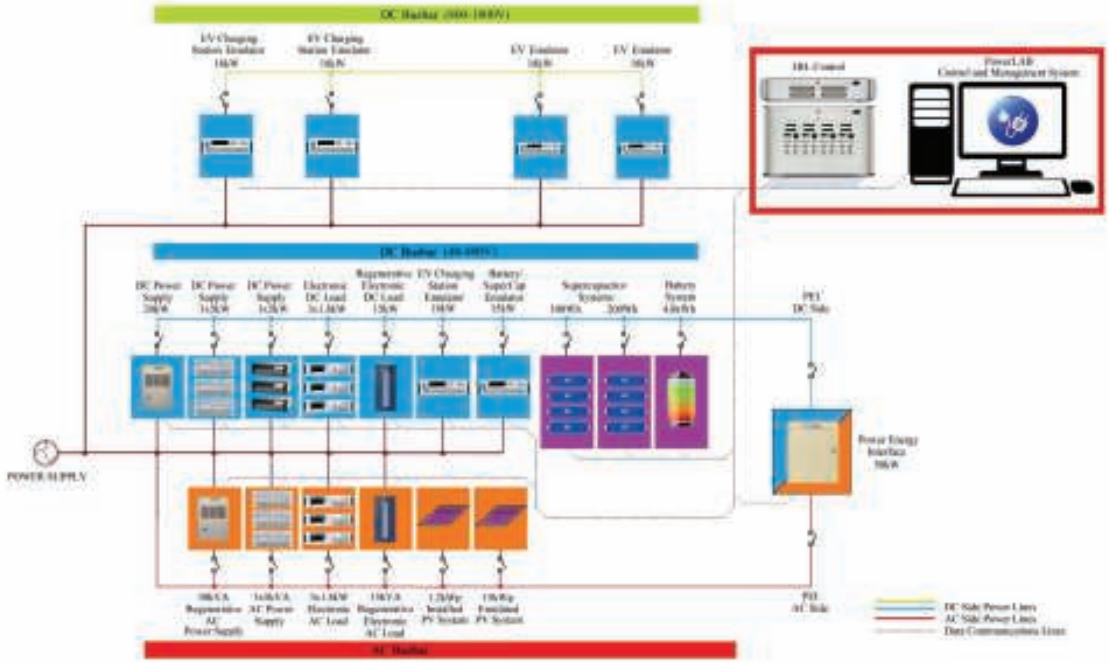

Fig. 1. Physical architecture of the lab microgrid facility.

- The state of the meters;
- The measurements produced.

B. Upper layer

This layer groups three components. The energy management & ancillary services component allows the creation and application of management policies to the grid, by means of the control centre. It includes ancillary services such as frequency resynchronization with the main grid resuming from an islanded state. It may request forecasting and multi-objective optimisation for its operation, and it archives and retrieves data relating to the control strategies of the microgrid. The command management services component enables the grid to be manually configured by means of the control centre. The status management services component manages the status information of both the instruments and the meters in the network, by means of the control centre. The energy and the command management services components provide configuration functionalities to the electrical network, whereas the status management services component enables its monitoring.

All the services components can communicate specific needs to the central controller for accessing the physical units without having to deal with the network infrastructure. Based on the requirements, synchronous (e.g., REST API) or asynchronous (e.g., publish/subscribe PUB/SUB protocols) communication can be adopted between upper and middle layer components. Relying on the services in the upper layer, advanced management services can be created, to allow for example the test of specific scenarios of the MG and experiment on the control strategies designed, as depicted in Fig. 3.

C. Bottom layer

All the controllers of the physical devices pertain to this layer. The local controllers exchange information with the central controller. Each controller manages a queue of commands received from the control centre that feeds to the instruments. They possibly use different protocols to interface with the instruments. The associated queue is also meant to store the output of the instruments (status, measurement) that will not be lost in case of communication faults. An instrument refers to an actual energy equipment that is configurable and emulates generation, load or energy storage. Controllers enable the network to rapidly adapt to changes such as physical unit losses or reconnections.

The protocols bus is a virtual channel where all the communications between the controllers and the instruments flow. Controllers may use several adapters or drivers for the communication, depending on the protocol adopted by the instrument, e.g. TCP, UDP, MODBUS (the list could be extended to IEC 61850, DNP3, CAN and other protocols).

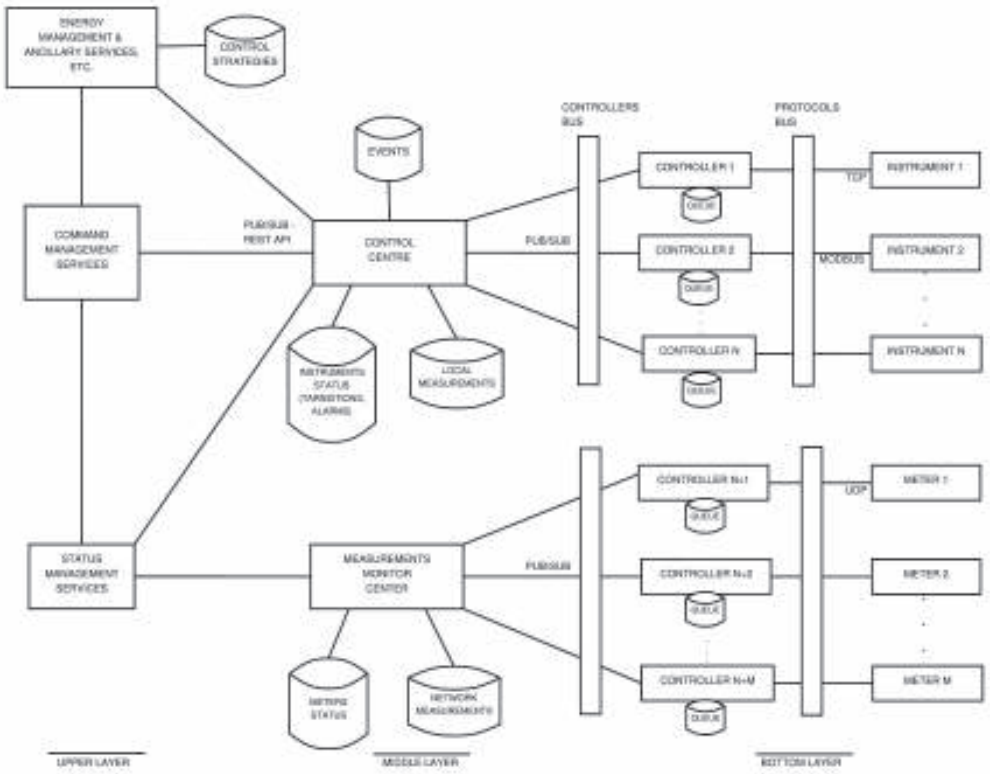

Fig. 2. Architecture of the management system for the lab microgrid facility: components and communications.

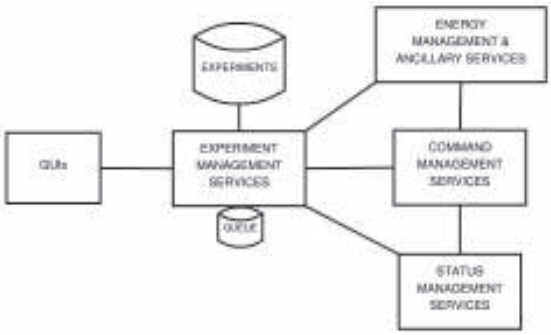

Fig. 3. Integration with the designed architecture of services for carrying out experiments on the MG.

The controllers bus is a virtual channel where all the communications between the control centre and the controllers flow. To interface with the local controllers, the control centre could use a PUB/SUB event-based protocol (e.g., MQTT, DDS, AMQP): the control centre publishes the control actions and the controllers subscribe to receive them. In turn, the control centre subscribes to the controller to receive data from it. The PUB/SUB pattern seems suitable for this role as it could manage all the requests in an asynchronous way, allowing a more efficient management of the requests load.

Analogue considerations applies to the communication in the measurements monitor side.

The use of queues and the proper use of the communication protocols selected can contribute to a more reliable communication in the network. PUB/SUB protocols indeed can be used to know the connection status in real time thanks to events. In addition, services in the upper layer needs to be protected (for example replicated) to enforce continuity of the network service.

IV. Case Study

For the sake of testing the proposed architecture, an experiment was carried out consisting of an advanced control logic aiming to avoid congestion issues while improving reliability of the lines of hybrid AC/DC MGs. A prototype system was implemented in Python to reproduce a simplified version of the communication architecture, and it was operated tailoring the physical architecture to the instrumentation needed.

Standard SCPI commands were used to pass setpoints to the instruments. To this aim a specific control logic — previously proposed in [7] and developed under the Project 2.7 funded by the Research Fund for the Italian Electrical System under the Contract Agreement "Accordo di Programma 2019-2021" between ENEA and the Ministry of Economic Development — was implemented into the PowerLab MG. In particular, the MG was configured according to the architecture shown in Fig. 4 both to show the flexibility of the platform to be adapted for testing different grid configurations and to verify the experimental results by comparing them with the simulated ones.

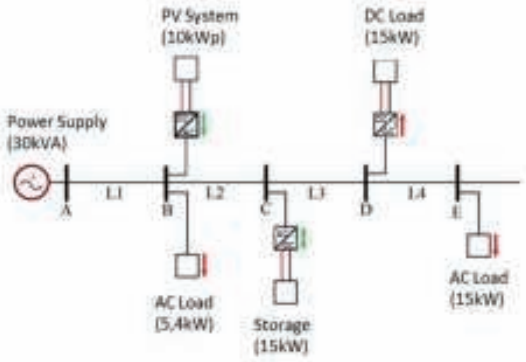

Fig. 4. PowerLab MG configuration for testing.

The architecture included: 4 lines L1, L2, L3 and L4, characterised by different lengths (from ten to one hundred of meters) and sections (starting by 4mm^2 to 16mm^2), 1 Li-Ion Battery (15 kW) coupled with a bi-directional DC/AC converter, 1 DC Load coupled with a DC/AC converter, 2 AC Loads (5,4 kW and 15 kW), 1 PV System (10 kWp), 1 Power Supply for grid emulation. The electrical cable coils, with different lengths and sections, are hosted in a dedicated rack connected with the PowerLab MG through contactors managed by a centralised system (PowerLab Management System). The tested control strategy aimed to avoid congestions issues during the operation of the hybrid MGs, while improving reliability of lines included into them. The test, in particular, consisted in emulating a congestion event by overloading the line L4 (at time steps 52–53) through ad-hoc time series for load and generation resources connected to the MG. L4 test horizon-time was equal to 24 h with a time step equal to 15 min. When the congestion occurred, the PowerLab Management System properly detected the anomaly (i.e., energy meters measured a line overcurrent greater than 90% of line loading) and activated the related control by sending signals to change the setpoint of the active power of the MG resources, according to the values assessed by the control. The measurements from the energy meters integrated into the physical MG (one energy meter per resource) are plotted below in Fig. 5, 6, 7. The results obtained were comparable with the simulation ones (deviation: 1%) and show the capability of the control both to solve congestions (in Fig. 5 the Line L4 Loading is lower than threshold after the control action) and improve reliability of the lines (the improvement, evaluated according to the methodology proposed in [7], is shown in 6). Finally, Fig. 7 shows how the control is able to decrease temperature rises for each grid line, especially in the case of congested lines where temperature decrease is approximately 5 °C thanks to the action of the control.

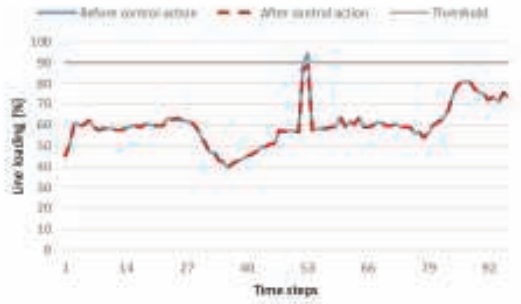

Fig. 5. Max line loading per each time step before and after the control action.

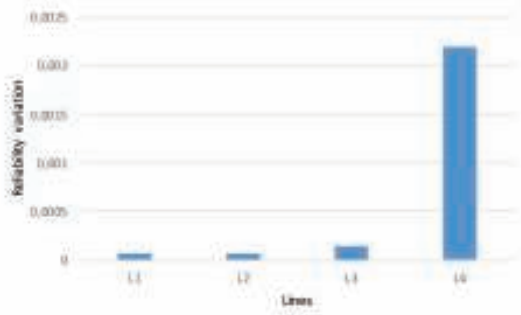

Fig. 6. Line reliability variation after the control action.

V. CONCLUSION AND FUTURE WORK

A lab-scale architecture was designed from the physical and communication sides to emulate microgrids containing renewable sources. The flexible architecture proposed can be adapted to test different control schemes and energetic scenarios. Also, it is scalable for the possibility to embed AC/DC power devices with different interfaces as well as extend its computational capacity. A control system prototype was then implemented using open source tools, to validate an advanced control logic aiming to avoid congestions while improving reliability for the microgrid. This software architecture will be

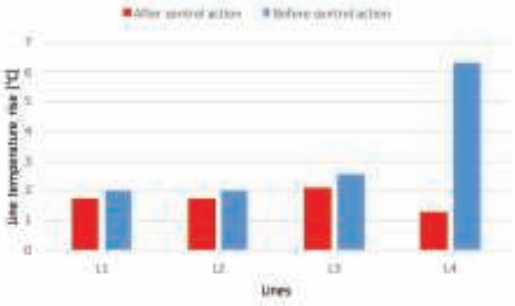

Fig. 7. Line temperature rise comparison.

further developed to enable researchers explore more complex scenarios.

ACKNOWLEDGMENT

The authors would like to acknowledge the Research Fund for the Italian Electrical System for funding this work through the project "Accordo di Programma 2019–2021 PTR_19_21_ENEA_PRG_10" between ENEA and the Ministry of Economic Development.

REFERENCES

[1] K. Hou, P. Tang, Z. Liu, H. Jia, and L. Zhu, "Reliability assessment of power systems with high renewable energy penetration using shadow price and impact increment methods," *Frontiers in Energy Research*, vol. 9, p. 23, 2021.

[2] I. Zenginis, J. Vardakas, C. Echave, M. Morato, J. Abadal, and C. Verikoukis, "Cooperation in microgrids through power exchange: An optimal sizing and operation approach," *Applied Energy*, vol. 203, pp. 972–981, 10 2017.

[3] Y. Li, T. Zhao, W. Ping, G. Beng, L. wu, and J. Ye, "Optimal operation of multi-microgrids via cooperative energy and reserve scheduling," *IEEE Transactions on Industrial Informatics*, vol. PP, 12 2017.

[4] A. S. Vijay, S. Doolla, and M. C. Chandorkar, "Real-time testing approaches for microgrids," *IEEE Journal of Emerging and Selected Topics in Power Electronics*, vol. 5, no. 3, pp. 1356–1376, 2017.

[5] https://www.typhoon-hil.com/solutions/microgrids/, 2021.

[6] M. Caliano, A. Buonanno, G. Graditi, A. Pontecorvo, G. Sforza, and M. Valenti, "Consumption based-only load forecasting for individual households in nanogrids: a case study," in *2020 AEIT International Annual Conference (AEIT)*, 2020, pp. 1–6.

[7] G. Adinolfi, R. Ciavarella, G. Graditi, A. Ricca, and M. Valenti, "A planning tool for reliability assessment of overhead distribution lines in hybrid ac/dc grids," *Sustainability*, vol. 13, no. 11, 2021.

[8] S. K. Sahoo, A. K. Sinha, and N. K. Kishore, "Control techniques in ac, dc, and hybrid ac–dc microgrid: A review," *IEEE Journal of Emerging and Selected Topics in Power Electronics*, vol. 6, no. 2, pp. 738–759, 2018.

[9] D. E. Olivares, A. Mehrizi-Sani, A. H. Etemadi, C. A. Cañizares, R. Iravani, M. Kazerani, A. H. Hajimiragha, O. Gomis-Bellmunt, M. Saeedifard, R. Palma-Behnke, G. A. Jiménez-Estévez, and N. D. Hatziargyriou, "Trends in microgrid control," *IEEE Transactions on Smart Grid*, vol. 5, no. 4, pp. 1905–1919, 2014.

[10] M. Roman-Barri, J. Cairo-Molins, A. Sumper, and A. Sudria-Andreu, "Experience on the implementation of a microgrid project in barcelona," in *2010 IEEE PES Innovative Smart Grid Technologies Conference Europe (ISGT Europe)*, 2010, pp. 1–7.

[11] A. Cagnano, E. De Tuglie, and L. Cicognani, "Prince — electrical energy systems lab: A pilot project for smart microgrids," *Electric Power Systems Research*, vol. 148, pp. 10–17, 2017.

[12] M. Restrepo, C. A. Cañizares, J. W. Simpson-Porco, P. Su, and J. Taruc, "Optimization- and rule-based energy management systems at the canadian renewable energy laboratory microgrid facility," *Applied Energy*, vol. 290, p. 116760, 2021.

[13] L. Meng, M. Savaghebi, F. Andrade, J. C. Vasquez, J. M. Guerrero, and M. Graells, "Microgrid central controller development and hierarchical control implementation in the intelligent microgrid lab of aalborg university," in *2015 IEEE Applied Power Electronics Conference and Exposition (APEC)*, 2015, pp. 2585–2592.

[14] A. Merabet, K. Tawfique Ahmed, H. Ibrahim, R. Beguenane, and A. M. Y. M. Ghias, "Energy management and control system for laboratory scale microgrid based wind-pv-battery," *IEEE Transactions on Sustainable Energy*, vol. 8, no. 1, pp. 145–154, 2017.

[15] M. Prodanovic, A. Rodriguez-Calvo, M. Jiménez-Carrizosa, and J. Roldán-Pérez, "A rapid prototyping environment for dc and ac microgrids: Smart energy integration lab (seil)," in *2017 IEEE Second International Conference on DC Microgrids (ICDCM)*, 2017, pp. 421–427.

[16] A. Colet-Subirachs, A. Ruiz-Alvarez, O. Gomis-Bellmunt, F. Alvarez-Cuevas-Figuerola, and A. Sudria-Andreu, "Centralized and distributed active and reactive power control of a utility connected microgrid using iec61850," *IEEE Systems Journal*, vol. 6, no. 1, pp. 58–67, 2012.

[17] R. Zamora and A. K. Srivastava, "Controls for microgrids with storage: Review, challenges, and research needs," *Renewable and Sustainable Energy Reviews*, vol. 14, no. 7, pp. 2009–2018, 2010.

3.4 A Simulation Analysis for Assessing the Reliability of AC/DC Hybrid Microgrids – Part I: Underground Station and Car Parking

A Simulation Analysis for Assessing the Reliability of AC/DC Hybrid Microgrids – Part I: Underground Station and Car Parking

Antonio Boni, Salvatore Favuzza, *Senior Member*, IEEE, Mariano Giuseppe Ippolito, Fabio Massaro, Salar Modari, Rossano Musca, Vincenzo Porgi, Gaetano Zizzo, *Senior Member*, IEEE,
Engineering Department
University of Palermo
Palermo, Italy

***Abstract*—This paper reports the results of a simulation study with the aim of evaluating the capability of two portions of a hybrid AC/DC MV/LV network of maintaining their operation in off-grid mode during the loss of the main AC grid due to a failure. In particular, the study aims to verify, in the case of islanded operation of the two microgrids, the continuity of the electricity service by exploiting the local generation plants, Energy Storage Systems (ESSs), and other flexible resources managed by suitable algorithms in different energy scenarios. The analysis was carried out considering two microgrids: an underground station and a car parking with Electric Vehicles (EVs). For assessing the performance of the network, specific indicators have been defined and calculated.**

***Keywords*—AC/DC microgrids; continuity; security; reliability; flexibility.**

I. INTRODUCTION

In the last decade, the scientific community has demonstrated an increasing interest in the concept of DC and hybrid AC/DC microgrids.

In [1], the authors present an exhaustive review of the power architectures, applications, and standardization issues for DC microgrids. In [2], the control strategies and stabilization techniques of such kinds of microgrids are analyzed. Also in [3], the authors face the problem of voltage control and energy management strategy of active distribution systems with a grid-connected DC microgrid as well as for an islanded DC microgrid with hybrid energy resources. In [4], an application of multilevel DC microgrids to residential buildings is presented, showing a method for optimizing the efficiency of DC/DC converters in parallel. In [5], a new and more flexible architecture for hybrid AC/DC microgrids with a multiport interlinking converter is proposed. Finally, in [6], a solar photovoltaic-battery energy storage-based microgrid with a multifunctional voltage source converter is presented. The above-cited papers represent only a small sample of the wide recent literature on the topic.

According to a meaningful increase in reliability and availability of the networks in both customer and operators point of view, one interesting aspect of hybrid AC/DC and DC microgrids is to investigate their reliability and their capability of ensuring service continuity in case of loss of the main AC supply. With this aim, the project "2.7 Modelli e strumenti per incrementare l'efficienza energetica nel ciclo di produzione, trasporto, distribuzione dell'elettricità", in the framework of the Research on Power Systems PTR 2019-2021 program, is currently examining various microgrids in order to collect useful information on these aspects. Considering previous studies and this paper, one topic appearing worthy to be investigated is how local generators, especially those based on Renewable Energy Sources (RES), ESSs, both stationary and for mobility, and flexible resources can contribute to the islanded operation of specific hybrid AC/DC microgrids.

In particular, in this paper, the authors analyze the impact of different energy scenarios on two hybrid networks: an underground station and a car parking with charging stations for EVs, in terms of the possibility of maintaining the continuity of supply for a given time. It is worth underlying that the study considers a very particular case: microgrids, operating in island mode due to a fault, are not equipped with specific devices for emergency power supply. What the study wants to investigate is, if it is possible and under such hypotheses, maintaining a microgrid with specific features in operation mode during a fault with only its local resources, and increasing the reliability for power supply of its loads. the second challenge that this study aims to address is: an increase in the number of RESs and ESSs can impact the results of such an analysis. Indeed, greater penetration of generating plants that exploit RESs, but also controllable loads, storage systems, and devices that are capable of implementing demand response actions, are expected in the next decades.

In [6], the authors investigated experimentally the feasibility of a smooth transition from grid-connected to stand-alone mode of a microgrid via a suitable control algorithms and presented a simple case with a storage system and a PV system. The present study investigates the possibility of such a transition from an energy point of view. As a first step, five different energy scenarios are defined based on the last reports of Terna, WEC, REN21, ENTSO-E, and other prominent organizations [7]-[11]. Then, four different microgrids are chosen and analyzed, showing the different behavior depending on the flexible resources and generators available: Photovoltaic (PV) and wind generators, controllable loads, static storage units, EVs and charging stations using V2G technology. Finally, some indicators defined by the same authors are calculated for assessing the reliability of each microgrid during a specific fault event.

The four microgrids considered in this study are: an underground station; a car parking with EV charging stations; a residential area downstream a distribution substation; a port area. In this paper, the first two areas are examined while the residential area and the port area are discussed in [12].

II. THE HYBRID AC/DC MICROGRIDS

The hybrid network of the Underground station (Fig. 1) is supplied by a 20 kilo volts AC grid and characterized by various voltage levels. An AC/DC converter provides DC

This research was funded by the Research Fund for the Italian Electrical System under the Contract Agreement "Accordo di Programma 2019-2021 – PTR_19_21_ENEA_PRG_10" between ENEA and the Ministry of Economic Development. Progetto 2.7.

978-1-6654-3613-7/21/$31.00 ©2021 IEEE

supply to the traction services; a MV/LV transformer supplies the 400 volts bus for the underground station services; a further AC/DC converter allows the supply of DC loads and the connection of a PV plant and storage units. The loads in the microgrid is comprised of lighting, ventilation, air conditioning, shops, etc.

The second microgrid, represented in Fig. 2, is that of a car parking. The grid is supplied by the public 20 kilo volts distribution grid by an MV/LV transformer. It has some AC loads (lighting, security point, video surveillance, electric gate, external lighting, etc.), and a DC bust connecting fast-charging stations for EVs, a PV system, and an energy storage system. The daily production profiles of the PV plants in the microgrids, expressed in p.u. of the rated power, are shown in Fig. 3. For their construction, the historical production data for the Italian territory in 2020 were considered [11]. The generation profile, on an hourly basis, of the individual generators present in the two microgrids were then obtained by defining the rated power of the generators for each scenario multiplied by the profiles in Fig. 3.

The size of the stationary ESS was estimated by applying the following steps;

- 1st Step: the base energy scenario (2020) is considered, and the daily production and consumption profiles are defined for each area. While the production profile is calculated as described above, and the daily consumption profiles are estimated from previous studies for each case study;

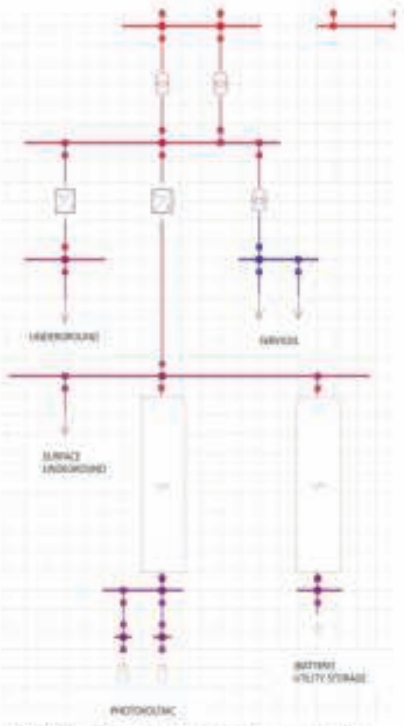

Fig. 1. Hybrid AC/DC microgrid of the underground station.

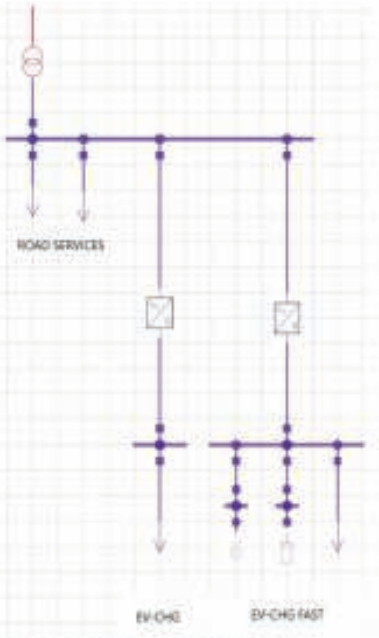

Fig. 2. Fig. 2. Hybrid AC / DC network of the Parking Area

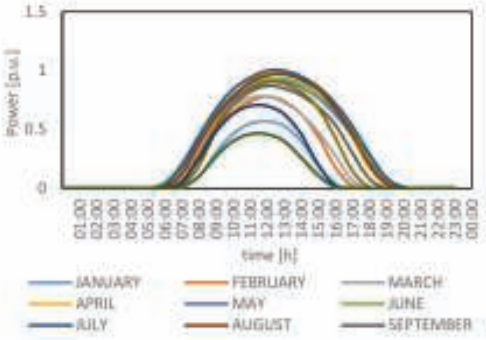

Fig. 3. Average monthly photovoltaic production in per unit (p.u).

- 2nd Step: the difference between generation and consumption is calculated. The production/consumption profiles are built on a quarter-hour basis and, consequently, the different will appear as a row vector, called "difference vector", consisting of 96 elements indicative of the average difference between the two profiles (production and consumption) for each 15 minutes-time interval;
- 3rd Step: the minimum value of the difference vector is found;
- 4th Step: the size of the static storage system is calculated considering the commercial size immediately higher than the minimum value extracted from the difference vector and increased by 30%; the capacity of the battery is calculated assuming type 2C batteries.

The above procedure for calculating the rated power and capacity of the energy storage was necessary because in all

the energy scenarios deduced from the examined reports, although storage systems installation trend is clearly declared in constant increase, it seems never reaching values suitable for the aim of this study. The above-described procedure appeared to be a good compromise for increasing the power and capacity of the storage units present in the microgrid, and at the same time, maintain these quantities far from those that would have characterized a storage system working as an emergency power supply.

Regarding the load, for the underground station, the load profile (Fig. 4) for each month were obtained by the study presented in [13], where the authors carry out a monthly-based evaluation of the energy consumption of an underground station with an extension of approximately 3000 m² and an annual influx of approximately 5.3 million passengers. The profiles shown in Fig. 4 only considers the electricity consumption attributable to the typical systems present in a station, such as: lighting, air conditioning, ventilation, video surveillance, etc., neglecting the consumption of the section devoted to the electric traction, since this was assumed to be supplied by the other underground station of the same line.

On the other hand, regarding the car parking, once the typical systems present in this area were defined (for example public lighting, signaling and video surveillance systems, etc.) an analysis of the charging profile was carried out considering typical occupancy profiles varying with seasons and the days of the week (weekdays and weekend); therefor, the charging profile of EVs is illustrated in Fig. 5. For the recharging section, to represent a more realistic condition with regards to the number of EVs connected to the electricity network, the study in [14] presents a percentage estimation for EVs connected to the grid during the different hours of a day.

According to the methodology described for calculating the features of the storage units, Fig. 6 and Fig. 7 show the daily trends of generation, consumption and the different vector for the underground station and car parking respectively, referred to the 2020 energy scenario, characterized by a lower penetration of distributed resources. In this energy scenario, the capacity of the static storage system was determined equal to 500 kWh for the metropolitan area and 25 kWh for the car parking area.

Starting from the data reported in [7]-[10], finally, the scenarios for the simulations are defined (Table I and Table

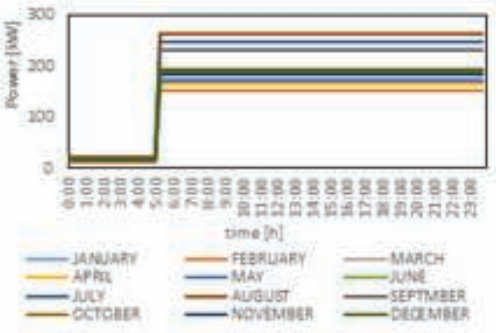

Fig. 4. Daily load profile of the underground station.

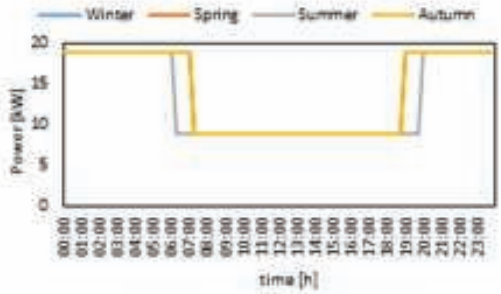

Fig. 5. Typical EVs' daily charging profile in the car parking for various seasons, variable consumption of EVs is excluded.

II) for both microgrids. Scenario 2020 is the base scenario. Scenarios 2030BC and 2030DEC are two different projections of the energy scenario in 2030, based on the analysis made by Terna and Snam [9]. Analogously two different future scenarios for 2040 are defined.

III. METHODOLOGY

The methodology implemented to assess the reliability of hybrid AC/DC microgrids is the following.

Firstly, it is assumed that a failure event occurs, causing the loss of supply from the main grid, and finally leads to operation of the microgrid in islanded mode. According to the last data from the Italian Regulatory Authority for Energy, Networks and the Environment (ARERA), the average duration of the fault is assumed 45 minutes [15].

By a Monte Carlo-like approach, the time interval in which the fault occurs is randomly drawn within the 96 15 minutes-time intervals of the day. Similarly, months of the year and days of the week are drawn.

On the basis of this information (months, days of the week, time in which the fault occurs) the daily load profiles and the daily production profile of the PV system to be used in the simulations are selected within those available. In presence of storage units and EVs, the number and type of EVs (V1G or V2G) and the State of Charge (SoC) of all the

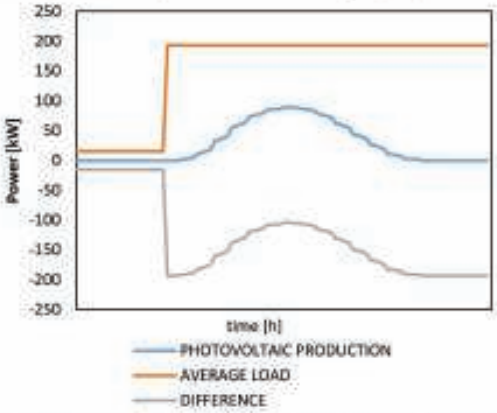

Fig. 6. Average profile of load, production and energy balance of the underground station in the 2020 energy scenario.

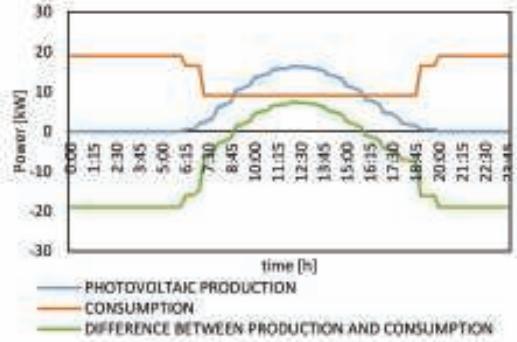

Fig. 7. Average profile of load, production and energy balance of the car parking in the 2020 energy scenario.

TABLE I. UNDERGROUND STATION: ENERGY SCENARIOS

	SCENARIO				
	2020	2030 BC	2030 DEC	2040 BC	2040 DEC
Daily energy consumption [kWh]	3694	3694	3694	3694	3694
PV system rated power [kW]	109	130	170	175	175
Electric energy storage rated power [kW]	250	250	250	250	250
Electric energy storage capacity [kWh]	500	500	500	500	500

TABLE II. CAR PARKING: ENERGY SCENARIOS

	SCENARIO				
	2020	2030 BC	2030 DEC	2040 BC	2040 DEC
Daily energy consumption [kWh]	653.5	973.5	973.5	1993	1993
PV system rated power [kW]	20	35	45	90	120
Electric energy storage rated power [kW]	25	25	25	25	25
Electric energy storage capacity [kWh]	50	50	50	50	50
V1G EV [n]	5	10	10	25	25
V2G EV [n]	5	10	10	25	25

batteries are drawn too. Particular attention has been paid to the SoC of the EVs' batteries for which the probability of being in charging at a given time of the day must be taken into account [14].

As soon as all the data of the system are known, it is assumed that all flexible resources and generators are managed by the energy management system of the microgrids to maximize the time for which the microgrids can operate in islanded mode. For doing this:

- generators are controlled in order to regulate voltage and frequency and supply the load;
- battery storage systems can behave as generators or loads depending on the difference between production and consumption in the microgrid. The SoC must be always included in the range 10%-90%, outside this range the battery enters the stand-by mode;
- interruptible loads are disconnected;
- flexible loads are shifted in time if generators are not able to supply the other loads. V2G EVs are considered as modulable loads/generators if the SoC allows the implementation of supporting the microgrid during the islanded operation, while V1G EVs are considered interruptible loads, if necessary.

In the various energy scenarios, the above quantities are present with different entities, and this influences the outcome of the assessment. Therefore, a system which is not able to maintain the stand-alone operation in the 2020 scenario could be able to do it in the 2040DEC.

Since the instant in which the fault influences the difference between production and consumption, the number of EVs connected to the grid and their SoC, and the other parameters impacting the assessment, various simulations must be carried out and the most significant one must be identified in order to clearly describe the behavior of the stand-alone system.

For doing this, the two networks were simulated in Matlab/Simulink environment together with the control algorithms for loads, generators, and storage units.

IV. RESULTS OF THE SIMULATIONS

A large number of simulations was done for the two microgrids. Three simulations have been chosen for each microgrid based on the rate between production and generation and on the presence of flexible resources. For the three simulations, table III indicates the capability of each microgrids to ensure operating in islanded mode during a 45-minute fault event: number 1 marks microgrids are able to operate in off-grid mode, and number 0 means they can not have a reliable operation during the fault event.

Table III reports only two cases for the underground station microgrid: 2020 and 2040DEC. The results for the other scenarios are not present since all scenarios for this microgrid are quite similar in which the microgrid may not operate in off-grid mode after the fault event (binary variable is 0).

Below two examples of calculation are reported, followed by the calculation of some general indicators for assessing the behavior of the microgrids.

Fig. 8 shows the results of one of the simulations carried out for the underground station microgrid. The loss of supply occurs at 18:00 and lasts 45 minutes. During this time range, the photovoltaic system present in the area produces a low amount of energy and is unable to guarantee the energy demand. The storage system delivers energy in the first 30 minutes before discharging. Because batteries in ESSs are able to supply only for 30 minutes, after 18:30 operator have

TABLE III. OUTCOMES OF THE SIMULATION

	UNDERGROUND STATION			*CAR PARKING*		
	S1	*S2*	*S3*	*S1*	*S2*	*S3*
2020	0	0	1	1	0	1
2030BC	-	-	-	1	1	1
2030DEC	-	-	-	1	0	1
2040BC	1	0	0	1	1	1
2040DEC				1	1	1

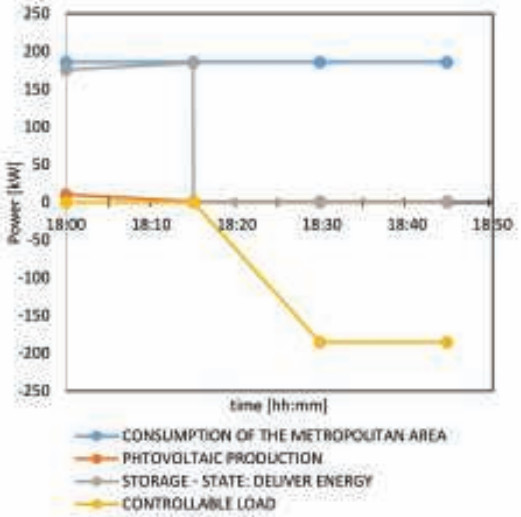

Fig. 8. Underground station: simulation results - Scenario 2020.

to start shedding loads sharply. Therefore, the microgrid is no more able to preserve its off-grid operation mode.

Fig. 9, analouglsy, shows the results of one of the simulations regarding the car parking microgrid during a loss of the main AC grid. The fault occurs in the MV network at 18:15. at 30-minutes duration of the fault, both PV system and ESS supply the demand electric power. at 18:40 batteries are depleted, and PV system is not able to generate enough power. this is the point where V2G EVs start delivering energy to the loads and compensate shortage power. therefore, in such circumstance, only V2G EVs can help in keeping the microgrid in stand-alone mode.

To quantify the reliability of the hybrid networks, some indicators have been defined. The first set of indicators is used for characterizing the microgrids in the various energy scenarios and during the failure event as follows:

- the *RES indicator* which evaluates the percentage of generation from renewable sources P_{RES} compared to the total power consumed in the examined area P_{load}:

$$RES = \frac{P_{RES}}{P_{load}} \cdot 100 \quad (1)$$

- the *FLEX indicator* that evaluates the flexibility of the load, i.e. the amount of energy that can participate at demand response (load shedding for example) $P_{LOAD,FLEX}$ divided by the total load:

$$FLEX = \frac{P_{load,flex}}{P_{load}} \cdot 100 \quad (2)$$

- the *BESS indicator* which evaluates the rate between the power supplied by the storage systems P_{BESS} and the total power consumed in the examined area:

$$BESS = \frac{P_{BESS}}{P_{load}} \cdot 100 \quad (3)$$

Another set of indicators was defined to quantify the impact that the individual energy scenarios have on the

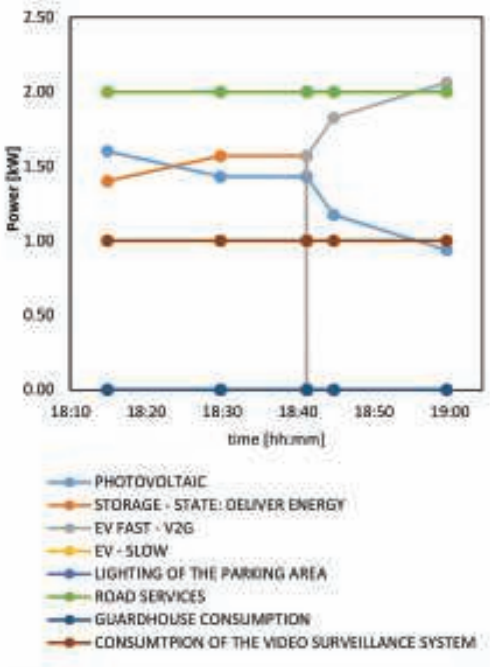

Fig. 9. Car Parking: simulation results - Scenario 2020.

safety of the electricity network examined. The first indicator is defined as "*the autonomy index of the microgrid*" which quantifies the islanding capacity of the microgrid upon the occurrence of a fault event. It is given by the rate between the duration of the stand-alone operation and the fault duration:

$$i_1 = \frac{h_i}{T} \cdot 100 \quad (4)$$

The second indicator is the "*flexibility index*" which quantifies the variation (increasing or decreasing) of active power available at the connection point between the islanded microgrid and the main network. It is given by:

$$i_2 = \frac{\Delta P_{load,flex} + \Delta P_{RES} + \Delta P_{BESS}}{A_n} \cdot 100 \quad (5)$$

where An is the rated power of the transformer at the point of common coupling between the two grids, and ΔP_{RES} , $\Delta P_{load,flex}$ and ΔP_{BESS} are, respectively, the average variation, during the fault, of the power generated by all RES plants, of the flexible load demand, and of the power delivered or consumed by the storage systems in the microgrid.

The last indicator is defined as "*the power profile modulation capacity index*" which evaluates the energy $\Delta E_{flex(T)}$ supplied by all the flexible resources present in the examined area compared to that theoretically available to keep the AC/DC network in stand-alone mode following the occurrence of the fault (E_{1h}):

$$i_3 = \frac{\Delta E_{flex(T)}}{E_{1h}} \cdot 100 \quad (6)$$

Table IV and V reports the calculation of the six indicators for the underground station and the car parking microgrids for the three most representative simulations.

TABLE IV. UNDERGROUND STATION: INDICATORS

SCENARIO 2020						
	RES	*FLEX*	*BESS*	i_1	i_2	i_3
1	2%	50%	48%	33%	47%	49%
2	1%	99%	0%	0%	41%	0%
3	65%	0%	35%	100%	41%	100%
SCENARIO 2040DEC						
	RES	FLEX	BESS	i_1	i_2	i_3
1	0%	0%	100%	100%	46%	100%
2	0%	50%	50%	33%	3%	50%
3	90%	10%	0%	0%	42%	0%

TABLE V. CAR PARKING: INDICATORS

SCENARIO 2020						
	RES	*FLEX*	*BESS*	i_1	i_2	i_3
1	36%	37%	44%	100%	2%	100%
2	4%	45%	25%	0%	3%	61%
3	100%	57%	0%	100%	4%	100%
SCENARIO 2030DC						
	RES	*FLEX*	*BESS*	i_1	i_2	i_3
1	178%	24%	0%	100%	8%	100%
2	2%	37%	98%	100%	7%	100%
3	0%	11%	100%	100%	2%	100%
SCENARIO 2030DEC						
	RES	*FLEX*	*BESS*	i_1	i_2	i_3
1	0%	28%	100%	100%	10%	100%
2	234%	4%	0%	67%	9%	100%
3	47%	18%	32%	100%	2%	100%
SCENARIO 2040DC						
	RES	*FLEX*	*BESS*	i_1	i_2	i_3
1	0%	28%	100%	100%	22%	100%
2	137%	30%	0%	100%	20%	100%
3	0%	21%	100%	100%	12%	100%
SCENARIO 2040DEC						
	RES	*FLEX*	*BESS*	i_1	i_2	i_3
1	100%	17%	0%	100%	13%	100%
2	158%	50%	0%	100%	20%	100%
3	0%	24%	100%	100%	17%	100%

By comparing the values assumed by the indicators of the first set with the capacity of the grid to operate in standalone mode for 45 minutes (results in Table III), it can be stated that the values of these indicators give precious indications on the flexible resources of the microgrids but they can't be put in relation with its reliability and with the continuity of the service.

The i_1 index has very variable values for all the simulations since it depends on the instant at which the fault occurs, the SoC of the batteries and, in general, the resources of the network. The car parking microgrid shows higher values of this indicator for almost all simulations. This is due to the lower load and to its low variability in time. The same analysis can't be said for the underground station.

i_2 is, in general, quite low (from 2% to 22%) and this indicates that in realistic scenarios like those considered in this work, the power variation at the point of common coupling is, in general, not significant.

Finally, i_3 is always high, showing that the considered microgrids can contribute to the main grid needs by modifying their consumption and increasing the grid reliability.

V. CONCLUSION

This work has presented a simulation analysis of the reliability of two microgrids investigating how the presence of flexible resources and local generators can increase the possibility of operating in stand-alone mode in case of loss of the main grid. Two sets of indicators have been calculated: the first one for characterizing the microgrid with regards to the presence of storage, flexible load, and RES generators, the second one for assessing its reliability. In general, it can be concluded that, in realistic scenarios based on the elaboration of the most recent projections of prominent energy and electrical organization, distributed flexible resources seems not to be able to support solely the operation of hybrid microgrids for more than 15-30 minutes (as an average), that is less than the average failure recovery time for Italian networks.

REFERENCES

[1] T. Dragicevic, X. Lu, J. C. Vasquez, J. M. Guerrero, "DC microgrids—part I: a review of power architectures, applications, and standardization issues", IEEE Transactions on Power Electronics, Vol. 31, No. 5, 2016, pp. 3528-3549.

[2] T. Dragicevic, X. Lu, J. C. Vasquez, J. M. Guerrero, "DC Microgrids—part I: a review of control strategies and stabilization techniques", IEEE Transactions on Power Electronics, Vol. 31, No. 7, 2016, pp. 4876-4891.

[3] S. Pannala, N. Patari, A. K. Srivastava, N. P. Padhy, "Effective control and management scheme for isolated and grid connected DC microgrid", IEEE Transactions on Industry Applications, Vol. 56, No. 6, pp. 6767-6780.

[4] V. Boscaino, J. M. Guerrero, I. Ciornei, L. Meng, E. Riva Sanseverino, G. Zizzo, "Online optimization of a multi-conversion-level DC home microgrid for system efficiency enhancement", Sustainable Cities and Society, Vol. 35, 2017, pp. 417-429.

[5] J. Khodabakhsh, G. Moschopoulos, "Simplified hybrid AC–DC microgrid with a novel interlinking converter", IEEE Transactions on Industry Applications, Vol. 56, No. 5, 2020, pp. 5023-5034.

[6] V. Narayanan, S.a Kewat, B. Singh, "Solar PV-BES based microgrid system with multifunctional VSC", IEEE Transactions on Industry Applications, Vol. 56, No. 3, 2020, pp. 2957-2967

[7] REN 21, «Renewables 2019 global status report,» REN 21, 2019.

[8] World Energy Council, "Energy storage monitor, latest trends on energy storage", WEC, 2019.

[9] Tema SpA, SNAM, "Documento di descrizione degli scenari 2019", 2019.

[10] ENTSO-E, ENTSOG, "TYNDP 2020, scenario report", 2020.

[11] Tema SpA, "Transparency Report", available at: https://www.tema.it/it/sistema-elettrico/transparency-report/actual-generation.

[12] A. Boni, S. Favuzza, F. Massaro, R. Musca, V. Porgi, G. Zizzo, "Analysis of Scenarios for Assessing the reliability of AC/DC hybrid Microgrids – Part II: Residential Area and Port Area", IEEE EEEIC/I&CPS Europe 2021, 7-10 October 2021, Bari (Italy).

[13] L. Lin, X. Liu, T. Zhang, X. Liu, "Energy consumption index and evaluation method of public traffic buildings in China", Sustainable Cities and Society, Vol. 57, 202 , article 102132.

[14] J. A. Peças Lopes, F. J. Soares, P. M. Almeida, M. Moreira da Silva, "Smart Charging Strategies for Electric Vehicles: Enhancing Grid Performance and Maximizing the Use of Variable Renewable Energy Resources", EVS24, 13-16 May 2009, Stavanger (Norway).

[15] ARERA, "Dati sulla continuità del servizio elettrico", https://www.arera.it/sas-frontend-cse/estrattoreLink".

3.5 A Simulation Analysis for Assessing the Reliability of AC/DC Hybrid Microgrids – Part II: Port Area and Residential Area

A Simulation Analysis for Assessing the Reliability of AC/DC Hybrid Microgrids – Part II: Port Area and Residential Area

Antonio Boni, Salvatore Favuzza, *Senior Member*, IEEE, Mariano Giuseppe Ippolito, Fabio Massaro, Salar Moradi, Rossano Musca, Vincenzo Porgi, Gaetano Zizzo, *Senior Member*, IEEE
Engineering Department
University of Palermo
Palermo, Italy

***Abstract*—This paper reports the second part of a simulation study with the aim of evaluating the ability of two portions of a hybrid AC/DC MV/LV network in maintaining their operation in off-grid mode during the loss of the main AC grid due to a failure. In particular, this paper follows a dual purpose: first, it analysis two microgrids in a residential area and a port zone capability of operating in islanded mode, applying a probabilistic approach, while there is different energy use cases, and second is to evaluate some reliability indicators.**

***Keywords*—AC/DC microgrids; continuity; security; reliability; flexibility.**

I. INTRODUCTION

In the last decade, the scientific community has demonstrated an increase in researchers' interest in the concept of DC and hybrid AC/DC microgrids.

In [1], the authors present an exhaustive review of the power architectures, applications, and standardization issues for DC microgrids. In [2], the control strategies and stabilization techniques of such kinds of microgrids are analyzed. Also in [3], the authors face the problem of voltage control and energy management strategy of active distribution systems with a grid-connected DC microgrid as well as for an islanded DC microgrid with hybrid energy resources. In [4], an application of multilevel DC microgrids to residential buildings is presented, showing a method for optimizing the efficiency of DC/DC converters in parallel. In [5], a new and more flexible architecture for hybrid AC/DC microgrids with a multiport interlinking converter is proposed. Finally, in [6], a solar photovoltaic/battery energy storage-based microgrid with a multifunctional voltage source converter is presented. The above-cited papers represent only a small sample of the wide recent literature on the topic.

In particular, in this paper, the authors analyze the impact that different energy scenarios have on the hybrid network of a residential and a port area with charging stations for Electric Vehicles (EVs), in terms of the possibility of maintaining the continuity of supply for a given time. It is worth underlying that the study considers a very particular case: the microgrids are operating in islanded mode due to a fault took place at AC main supply, and are not equipped with specific devices for emergency power supply. What the study wants to investigate is, if it is possible and under which hypotheses, preserving a microgrid with specific features in operation during a fault with only its own local resources, increasing the reliability for its demand supply. A second challenge that the study tries to tackle is: how an increase in RES and ESS capacity can impact the results of such an analysis. Indeed, greater penetration of generating plants that exploit RESs, but also controllable loads, storage systems, and devices which are capable of implementing demand response actions are expected in the next decades.

In [6], the authors investigated experimentally the feasibility of a smooth transition from grid-connected to stand-alone mode of a microgrid using suitable control algorithms and presented a simple case with a storage system and a PV generator. The present study investigates the possibility of such a transition from an energy point of view. As the first step, five different energy scenarios are defined based on the last reports of Terna, WEC, REN21, ENTSO-E and other prominent organizations [7]-[11]. Then, four different microgrids are chosen and analyzed, showing the different behavior of each grid, dependent on the flexible resources and generators available: Photovoltaic (PV) and wind generators, controllable loads, static storage units and, EVs, and charging stations using V2G technology. Finally, some indicators defined by the same authors are calculated for assessing the reliability of each microgrid.

The four microgrids considered in this study are an underground station, a car parking with EV charging stations, a residential area downstream of a distribution substation, and a port area. In this paper, the residential and the port area microgrids are examined while the results of the study of the first two networks are presented in [12].

II. THE HYBRID AC/DC MICROGRIDS

Fig. 1 and Fig. 2 show the residential area and the port area microgrids, respectively. To study the behavior of both networks, in a preliminary phase, it is necessary to define the load and generation profiles that characterize them.

For the residential network, the presence of a 400 kVA MV/LV secondary substation has been hypothesized with a daily load diagram with a seasonal variation like that present in [13]. As regards the port network, it was assumed a consumption daily profile with no seasonal or monthly variations, linked to the services present within the port and defined by the study carried out in [14].

In both microgrids, there are distributed generation nodes with PV and wind power plants. By consulting the data base of the "Transparency Report" platform of the Italian TSO Terna [11], it was possible to examine an hour-based daily electricity produced data in Italy divided per primary source.

Therefore, the energy produced by wind and PV plants for the year 2020, and the daily data for each month of the year were collected. Each generic value E_{ijk} of the database is a function of the i-th month, the j-th day, and the k-th hour, where:

This research was funded by the Research Fund for the Italian Electrical System under the Contract Agreement "Accordo di Programma 2019-2021 – PTR_19_21_ENEA_PRG_10" between ENEA and the Ministry of Economic Development. Progetto 2.7.

978-1-6654-3613-7/21/$31.00 ©2021 IEEE

- i = January, February,..., December;
- $j = 1, 2, \ldots, g_{max}$;
- k = 00:00, 01:00, ..., 24:00.

with:

$$g_{max} = \begin{cases} 29, \text{ for February} \\ 30, \text{ for April, June, September, November} \\ 31, \text{ for the other month} \end{cases}$$

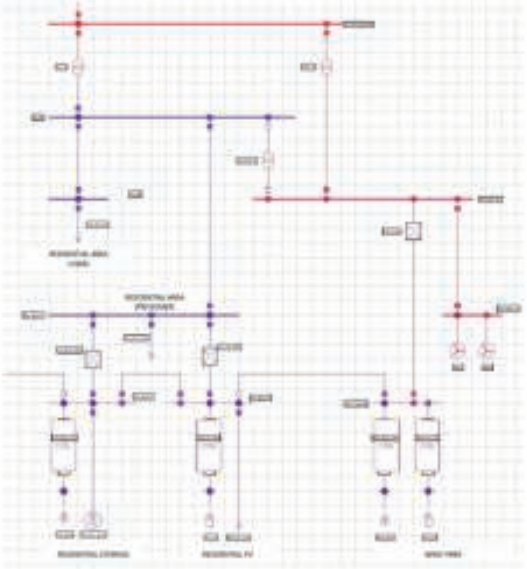

Fig. 1. Residential Area Network

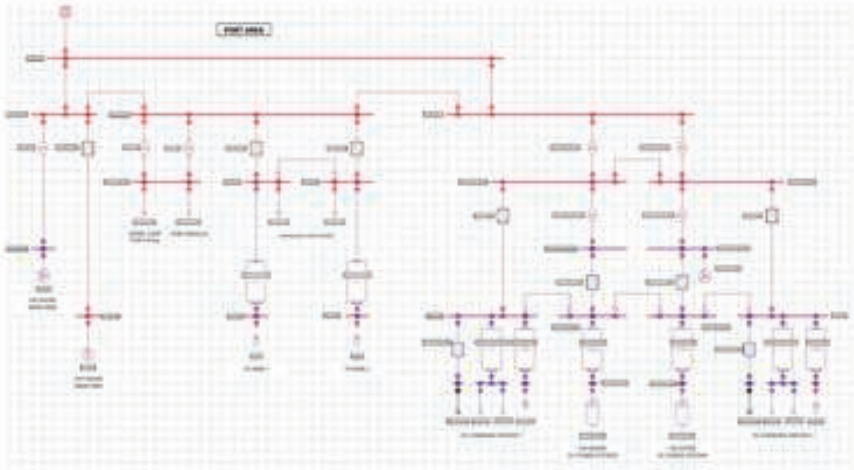

Fig. 2. Port Area Network

The energy values $E_{i,j,k}$ refers to one hour, therefore it is possible to consider it as a equivalent single value for the average active power $P_{i,j,k}$ produced at the given hour. Fig. 3 and Fig. 4 show respectively the daily photovoltaic and wind generation profiles (in per unit) obtained.

Within the port area microgrid, there is a parking lot with slow- and fast-charging stations for EVs. For the first type of charging station a maximum power of 3 kW has been assumed. These stations are considered as the interruptible loads in the microgrid. For fast-charging stations, the maximum power of 10 kW is assumed and along with EVs

are considered operating with V2G technology. The injection/consumption profiles of the EVs depend on the number of them connected to the network during the day and on the demand of the network [15].

As regards storage for the residential network and cold-ironing for the port network, the profiles vary according to the control logic applied and the microgrid load demand.

After extracting identified all power profiles in p.u., before proceeding with the simulations, it was necessary to identify, based on what was done in [12], the base values

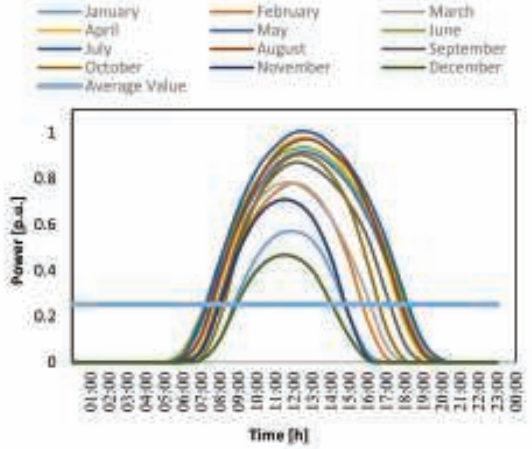

Fig. 3. Photovoltaic system power output expressed in [p.u.].

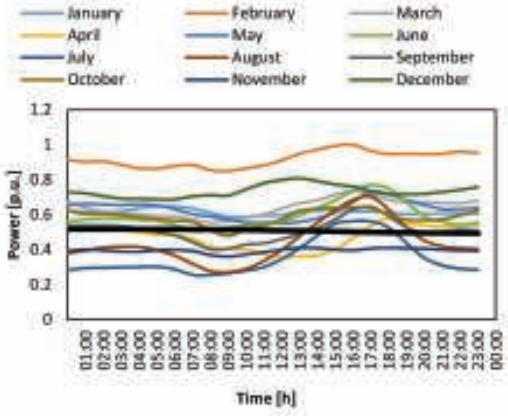

Fig. 4. Wind Farm power output expressed in [p.u.].

appropriately calculated for all the considered scenarios. In Table I, the base values deduced by [7]-[10] for the residential area microgrid for all scenarios are shown. In Table II, those related to the port area network are reported.

III. CALCULATION CODE

The model is implemented in the MATLAB environment and is based on a probabilistic Montecarlo-type approach, simulates the island operation of the considered networks by randomly choosing the month, day, and instant at which the failure occurs. Having such information, it was possible to select the generation and consumption profiles relevant to the assessment. Therefore, the analysis of the above-described networks focuses on the time interval between the instant of failure extracted and the final instant, calculated as follows:

$$final\ time\ of\ the\ fault = initial\ time\ of\ the\ fault + duration\ of\ the\ fault$$

where, the duration of the fault, according to [17], is assumed equal to 45 minutes for faults taking place in MV.

Depending on the time instant extracted, according to the profile in [16] concerning the percentage of EVs connected to the network during a typical day, it was possible to determine the number of fast-charging EVs and

TABLE I. BASE VALUES FOR THE RESIDENTIAL NETWORK.

	2020	2030 BC	2030 DEC	2040 BC	2040DEC
Residential Consumption [kWh]	3696.00	3991.68	4213.44	4287.36	4656.96
Peak Value [kW]	280.00	302.40	319.20	324.80	352.80
PV Rated Power [kW]	33.00	43.00	60.00	62.00	87.00
Wind plants Rated Power [kW]	33.00	43.00	60.00	62.00	87.00
Storage Power [kW]	270	300	290	290	310
Energy Storage capacity [kWh]	540	600	580	580	620
n. EVs (Fast Charge) [-]	5	10	10	10	10
n. EVs (Slow charge) [-]	5	10	10	10	10

TABLE II. BASE VALUES FOR THE PORT NETWORK

	2020	2030 BC	2030 DEC	2040 BC	2040DEC
Port Consumption [kWh]	48559.11	52443.83	55357.38	56328.56	61184.47
Peak Value [kW]	4000.00	4320.00	4560.00	4640.00	5040.00
Controlled Load [kW]	200.00	216.00	228.00	232.00	252.00
PV Rated Power [kW]	320.00	570.00	1000.00	830.00	1470.00
Wind plants Rated Power [kW]	550.00	550.00	550.00	800.00	800.00
Cold Ironing Power [kW]	2000.00	2000.00	2000.00	4000.00	4000.00
Cold ironing Energy [kWh]	4000.00	4000.00	4000.00	8000.00	8000.00
n. EVs (Fast Charge) [-]	5	10	10	25	25
n. EVs (Slow charge) [-]	5	10	10	25	25

slow-charging EVs connected to the network through the charging columns. For each of them, through the Monte carlo extraction, the State of Charge (SoC) has been defined on which the charge/discharge time depends, considering that the EVs operate with SoC values between 10% and 90% of total capacity. Knowing the charging and discharging times for each EV, and comparing them with the duration of the failure, it was possible to determine the profile of the fast-charging EVs and the slow-charging EVs within the fault time range, considering that, depending on the network requirement, the former can operate in V2G, while the latter

can operate as a flexible load to guarantee, where possible, island operation of the network and hence the balance between generated and absorbed active power. The same control logic was implemented with the storage present in the residential network and that of the ships connected with cold-ironing technology in the port network.

IV. RESULTS

The results obtained for all scenarios are shown below. According to the methodology explained in the first part of this study [12], various simulations were carried out for each scenario. Three of the most significant simulations (Simulations S1, S2, S3) are reported in the tables below. In particular, Table III indicates the capability of each microgrids to ensure operating in islanded mode during a 45-minute fault event: number 1 marks microgrids are able to operate in off-grid mode, and number 0 means they can not have a reliable operation during the fault event. Table IV, on the other hand, reports the minutes of the stand-alone operation for each simulation.

RES Index:

$$R\dot{E}S = \frac{P_{RES}}{P_{load}} \cdot 100 \quad (1)$$

where:

- P_{RES}: total power generated by all the RES generation plants present in the considered microgrid;
- P_{LOAD}: total load of the microgrid;

1) FLEX Index:

$$FLEX = \frac{P_{load,flex}}{P_{load}} \cdot 100 \quad (2)$$

where:

TABLE III. ISLANDING MODE INDEX

	RESIDENTIAL AREA NETWORK			PORT AREA NETWORK		
	S1	S2	S3	S1	S2	S3
2020	0	0	1	0	1	0
2030-BC	1	0	0	0	1	0
2030-DEC	0	0	1	0	0	0
2040-BC	0	0	0	0	0	0
2040-DEC	0	0	1	0	0	1

TABLE IV. RANGE TIME IN ISLANDING MODE

	RESIDENTIAL AREA NETWORK			PORT AREA NETWORK		
	S1	S2	S3	S1	S2	S3
2020	00:40	00:33	00:45	00:00	00:45	00:00
2030-BC	00:45	00:15	00:36	00:00	00:45	00:00
2030-DEC	00:21	00:09	00:45	00:00	00:00	00:00
2040-BC	00:25	00:38	00:16	00:00	00:00	00:27
2040-DEC	00:16	00:32	00:45	00:19	00:27	00:45

- $P_{load,FLEX}$ the total power of flexible loads of the microgrids;

2) BESS Index:

$$B\dot{E}SS = \frac{P_{BESS}}{P_{load}} \cdot 100 \quad (3)$$

where:

- P_{BESS} the total power supplied/consumed by all storage systems;

3) i_1 Index:

$$i_1 = \frac{h_i}{T} \cdot 100 \quad (4)$$

where:

- h_i: the time duration at which given microgrid can operatein islanded mode;
- T: failure duration;

4) i_2 Index:

$$i_2 = \frac{\Delta P_{load,flex} + \Delta P_{RES} + \Delta P_{BESS}}{A_n} \cdot 100 \quad (5)$$

where:

- A_n is the apparent power of the node to which the portion of the considered network is connected;
- ΔP_{RES} is the average variation, in the time interval of the failure, of the total power generated by all RES generation plants present in the microgrid;
- $\Delta P_{load,flex}$ is the average variation, in the time interval of the failure, of the total power of the flexible loads;
- ΔP_{BESS} is the average variation, in the time interval of the fault, of the total power delivered by the storage
- systems in the microgrid, required by the AC network.

5) i_3 Index:

$$i_3 = \frac{\Delta E_{flexe(T)}}{E_{th}} \cdot 100 \quad (6)$$

where:

- $\Delta E_{flexe(T)}$: energy supplied by the flexible devices present in the microgrid in the time interval of the fault;
- E_{th} : energy required to ensure island operation of the portion of the considered network in the time interval of the fault.

For each simulation and for each microgrid (residential and port area), the indicators are reported at Tables from V to XVI.

A. Residential Area Network

TABLE V. *RES* INDEX

Scenario	Simulation 1	Simulation 2	Simulation 3
2020	20%	35%	9%
2030 BC	10%	44%	16%
2030 DEC	33%	46%	9%
2040 BC	42%	52%	15%
2040 DEC	53%	61%	20%

TABLE VI. *FLEX* INDEX

Scenario	Simulation 1	Simulation 2	Simulation 3
2020	20%	33%	0%
2030 BC	0%	43%	43%
2030 DEC	33%	40%	0%
2040 BC	27%	12%	42%
2040 DEC	23%	12%	42%

TABLE VII. *BESS* INDEX

Scenario	*Simulation 1*	*Simulation 2*	*Simulation 3*
2020	60%	32%	91%
2030 BC	90%	14%	62%
2030 DEC	34%	14%	91%
2040 BC	31%	36%	43%
2040 DEC	24%	29%	80%

TABLE VIII. i_1 INDEX

Scenario	*Simulation 1*	*Simulation 2*	*Simulation 3*
2020	67%	33%	100%
2030 BC	100%	0%	33%
2030 DEC	33%	0%	100%
2040 BC	33%	67%	33%
2040 DEC	33%	67%	100%

TABLE IX. i_2 INDEX

Scenario	*Simulation 1*	*Simulation 2*	*Simulation 3*
2020	24%	31%	37%
2030 BC	32%	37%	59%
2030 DEC	24%	39%	68%
2040 BC	35%	41%	62%
2040 DEC	25%	45%	56%

TABLE X. i_3 INDEX

Scenario	*Simulation 1*	*Simulation 2*	*Simulation 3*
2020	76%	49%	100%
2030 BC	100%	24%	58%
2030 DEC	51%	26%	100%
2040 BC	53%	74%	53%
2040 DEC	53%	72%	100%

B. Port Area Network

TABLE XI. *RES* INDEX

Scenario	*Simulation 1*	*Simulation 2*	*Simulation 3*
2020	12%	36%	13%
2030 BC	22%	18%	27%
2030 DEC	29%	11%	25%
2040 BC	34%	44%	29%
2040 DEC	13%	57%	35%

TABLE XII. *FLEX* INDEX

Scenario	*Simulation 1*	*Simulation 2*	*Simulation 3*
2020	7%	22%	5%
2030 BC	6%	26%	7%
2030 DEC	20%	6%	5%
2040 BC	7%	29%	7%
2040 DEC	19%	9%	19%

TABLE XIII. *BESS* INDEX

Scenario	*Simulation 1*	*Simulation 2*	*Simulation 3*
2020	35%	42%	13%
2030 BC	30%	55%	65%
2030 DEC	8%	57%	45%
2040 BC	1%	22%	28%
2040 DEC	20%	13%	46%

TABLE XIV. i_1 INDEX

Scenario	*Simulation 1*	*Simulation 2*	*Simulation 3*
2020	0%	100%	0%
2030 BC	0%	67%	0%
2030 DEC	0%	0%	0%
2040 BC	0%	33%	33%
2040 DEC	33%	67%	100%

TABLE XV. i_2 INDEX

Scenario	*Simulation 1*	*Simulation 2*	*Simulation 3*
2020	6%	4%	5%
2030 BC	8%	4%	12%
2030 DEC	3%	11%	13%
2040 BC	6%	4%	9%
2040 DEC	4%	9%	6%

TABLE XVI. i_3 INDEX

Scenario	*Simulation 1*	*Simulation 2*	*Simulation 3*
2020	47%	100%	20%
2030 BC	52%	100%	98%
2030 DEC	43%	72%	68%
2040 BC	12%	91%	55%
2040 DEC	43%	59%	100%

Analyzing the data in Table III, it is possible to assert that: in 26.67% of the simulations carried out for the residential area network it is possible to keep islanded mode; and in 20% of the simulations carried out for the port network it is possible to keep islanded mode.

These low percentage values are justified by the fact that there are services/activities that have a daily load profile that changes with sudden variations over time and therefore difficult to feed through generation from RES and/or storage systems.

The contributions of RES, storage and flexible loads in the different energy scenarios from 2020 to 2040, on the other hand, seem to have an insignificant influence on the outcome of the simulations.

It is of particular interest to analyze the data in Table IV where, for all simulations, the time for which the network is able to maintain islanding is shown. Note is that, while the residential network is almost able to operate in off-grid mode even for a few minutes, in the simulations of the port network there is a clear cut so that the network is capable of preserving islanded mode for low number of simulations in the fault duration (only 20% of the simulations). This consideration is found to a lesser extent in the 2040-BC and 2040-DEC scenarios, where the growing size of storage, cold ironing and V2G EVs allow for greater load coverage. The result above is obviously reflected in the calculation of the indicators.

Also for these two microgrids, like for those examined in [12], the i_1 index shows its variability as a function of the instant in which the fault occurs, the availability of charge in the batteries, and, in general, of the resources of the network. The residential area microgrid shows higher values of this indicator for almost all simulations. This is due to the lower load. The same can't be said for the underground station.

i_2 is, in general, lower in the port area (from 3% to 13%) than in the residential area (from 24% to 68%) and this indicates that in realistic scenarios like those considered in this work, for the port area microgrid, the power variation at the point of common coupling is, in general, not significant.

Finally, i_3 is always high, showing that the considered microgrids can contribute to the main grid needs by modifying their consumption and increasing the grid reliability.

Finally, it is important to underline that in order for DC microgrids to be effectively able to improve the reliability of

a distribution system, a technological leap is necessary regarding the introduction in networks such as reliable supervision and control systems, reclosure systems rapid backup lines, electronic DC / DC and DC / AC converters which are capable of being totally enslaved by the island's Energy Management System in order to guarantee the operation of the network.

All of this is still under study and is a central theme of research on Smart Grids and the Electrical System.

V. Conclusion

The present work has been carried out in the framework of the project "2.7 Modelli e strumenti per incrementare l'efficienza energetica nel ciclo di produzione, trasporto, distribuzione dell'elettricità", PTR 2019-2021. The paper has presented a simulation analysis of the reliability of two microgrids, investigating how the presence of flexible resources and local generators can increase the possibility of operating in stand-alone mode in case of loss of the main grid. Two sets of indicators have been calculated: the first one for characterizing the microgrids with regards to the presence of storage system, flexible load, and RES generators, the second one for assessing the microgrids reliability. In general, it can be concluded that, in realistic scenarios based on the elaboration of the most recent projections of prominent energy and electrical organization, distributed flexible resources seems not be able to support solely the operation of hybrid microgrids for more than 15-30 minutes (as an average), that is less than the average failure recovery time for Italian networks.

References

[1] T. Dragicevic, X. Lu, J. C. Vasquez, J. M. Guerrero, "DC microgrids—part I: a review of power architectures, applications, and standardization issues", IEEE Transactions on Power Electronics, Vol. 31, No. 5, 2016, pp. 3528-3549.

[2] T. Dragicevic, X. Lu, J. C. Vasquez, J. M. Guerrero, "DC microgrids—part I: a review of control strategies and stabilization techniques", IEEE Transactions on Power Electronics, Vol. 31, No. 7, 2016, pp. 4876-4891.

[3] S. Pannala, N. Patari, A. K. Srivastava, N. P. Padhy, "Effective control and management scheme for isolated and grid connected DC microgrid", IEEE Transactions on Industry Applications, Vol. 56, No. 6, pp. 6767-6780.

[4] V. Boscaino, J. M. Guerrero, I. Ciornei, L. Meng, E. Riva Sanseverino, G. Zizzo, "Online optimization of a multi-conversion-level DC home microgrid for system efficiency enhancement", Sustainable Cities and Society, Vol. 35, 2017, pp. 417-429.

[5] J. Khodabakhsh, G. Moschopoulos, "Simplified hybrid AC–DC microgrid with a novel interlinking converter", IEEE Transactions on Industry Applications, Vol. 56, No. 5, 2020, pp. 5023-5034.

[6] V. Narayanan, S.a Kewat, B. Singh, "Solar PV-BES based microgrid system with multifunctional VSC", IEEE Transactions on Industry Applications, Vol. 56, No. 3, 2020, pp. 2957-2967

[7] REN 21, «Renewables 2019 global status report,» REN 21, 2019.

[8] World Energy Council, "Energy storage monitor, latest trends on energy storage", WEC, 2019.

[9] Tema SpA, SNAM, "Documento di descrizione degli scenari 2019", 2019.

[10] ENTSO-E, ENTSOG, "TYNDP 2020, scenario report", 2020.

[11] Tema SpA, "Transparency report", available at: https://www.tema.it/it/sistema-elettrico/transparency-report/actual-generation.

[12] A. Boni, S. Favuzza, F. Massaro, R. Musca, V. Porgi, G. Zizzo, "Analysis of scenarios for assessing the reliability of AC/DC hybrid microgrids – part I: underground station and car parking", IEEE EEEIC/I&CPS Europe 2021, 7-10 October 2021, Bari (Italy).

[13] RSE, "Analisi di impatto dell'introduzione della tariffa biorario obbligatoria", Technical Report 13000580, 2012.

[14] G. Parise, L. Parise, L. Martirano, P. B. Chavdarian, Chun-Lien Su, A. Ferrante, "Wise port and business energy management: port facilities, electrical power distribution", IEEE Transactions on Industry Applications, 2015, 52.1: 18-24.

[15] L. Lin, X. Liu, T. Zhang, X. Liu, "Energy consumption index and evaluation method of public traffic buildings in China", Sustainable Cities and Society, Vol. 57, 202 , article 102132.

[16] J. A. Peças Lopes, F. J. Soares, P. M. Almeida, M. Moreira da Silva, "Smart charging strategies for electric vehicles: enhancing grid performance and maximizing the use of variable renewable energy resources", EVS24, 13-16 May 2009, Stavanger (Norway).

[17] ARERA, "Dati sulla continuità del servizio elettrico", https://www.arera.it/sas-frontend-cse/estrattoreLink/.

3.6 Development of an Energy Management System for AC/DC hybrid networks: from abstract functional requirements to the flexible tool

Development of an Energy Management System for AC/DC hybrid networks: from abstract functional requirements to the flexible tool

Davide Fioriti
DESTEC
University of Pisa
Pisa, Italy
davide.fioriti@ing.unipi.it

Giovanni Lutzemberger
DESTEC
University of Pisa
Pisa, Italy
giovanni.lutzemberger@unipi.it

Davide Poli
DESTEC
University of Pisa
Pisa, Italy
davide.poli@unipi.it

***Abstract*—Alternating Current (AC) networks are the predominant technologies used to transmit and distribute electricity worldwide. However, the penetration of renewable sources and the decreasing costs in power electronics are making Direct Current (DC) systems a promising approach to increase energy efficiency, reliability, and resilience, while exploiting synergies with AC systems. Therefore, appropriate Energy Management Systems (EMS) are mandatory for achieving energy efficiency and economic profitability, which shall account for both AC and DC components and networks. Moreover, in practical applications, multiple different control methodologies have been proposed to manage power systems, with different simulation tools, development platforms and software tools, which rarely have the same interface. This study aims at proposing the generalized framework and the tool for the development of a flexible EMS, which could be easily interfaced with standard commercial tools, e.g. NEPLAN or PowerFactory. The theoretical and functional requirements of the methodology can lay the foundations for further research studies and the proposed results confirm the robustness of the methodology.**

***Keywords*—Pyomo, Mixed-Integer Linear Programming (MILP), AC/DC hybrid energy systems, hybrid vehicles, abstract cyber modelling**

I. INTRODUCTION

The power system is evolving towards a higher penetration of renewable sources that are often non-dispatchable [1], [2], thus potentially leading to stability and reserve problems. In particular, the higher penetration of renewable assets may cause a progressive reduction in the use of fossil-fuel-based power generation, hence leading to less profitable investments and the possible commissioning of the traditional generation plants. However, these power plants are also the backbone for the power system stability, as they provide the main inertia to the system and reserve; thus innovative storage devices, control systems and energy recovery are needed to successfully meet the energy transition targets [1]–[3], according to the EU Clean Energy Package [4], [5].

Accounting for the uncertainties in both the load and the renewable production, the future energy grids shall provide flexibility and appropriate energy system control. In particular, appropriate Energy Management Systems (EMSs) shall be developed to properly operate portion of the grids with the goal of supporting and efficiently use the local renewable generation and storage. However, most renewable sources supply power at direct current (DC), while the traditional power system is based on alternating current (AC), therefore advanced controls and AC/DC converters are needed for the efficient and reliable use of energy. Therefore, EMSs shall properly operate mixed AC/DC systems.

The literature is rich in methodologies proposed to operate power systems and microgrids with the goal of minimising their operating costs [6]–[11]. However, the majority of the studies traditionally focuses on AC systems only or localized systems without accounting for a large area network [12]. Mixed AC/DC systems are quite common for power generating units where the DC node is used as common busbar for connecting renewable production and batteries; more rarely, mixed AC and DC networks are accounted for [13]. However, given the large use of DC power generating assets and Battery Energy Storage Systems (BESS), in the foreseeable future mixed AC and DC networks can be used also in Medium Voltage (MV) and Low Voltage (LV) networks [13]. For these reasons, the development of EMS methods accounting for general AC and DC networks is needed and discussed in this study.

Tackling the uncertainties in the system operation is very challenging and many approaches have been proposed [14]–[17]. Stochastic, Aggregating-Rule-based Stochastic Optimization (ARSO), robust, chance-constraint optimization are the main methodologies used for this purpose [18]. However, they require not only the forecast, but also an adequate calibration of the forecasting uncertainty that is not easy to accomplish; the computational requirements may be relevant, especially considering the traditional control hardware used in the power industry. More simple predictive methodologies, instead, may rely on a single forecast, but the forecasting and optimization process are run more frequently, e.g. infra-daily, to update the optimal system dispatching and promptly correct deviations from the expected operation.

In this regard, the research center ENEA, in collaboration with Italian Universities, has promoted research activities on future mixed AC and DC networks, accounting for decentralized energy resources, BESS and electric charging stations. The final goal of the activity is the development of a unique tool comprising the expertise of different partners, including the development of an EMS to be interfaced with general AC/DC networks loaded in commercial software for energy studies: NEPLAN [19] and PowerFactory [20]. Therefore, the EMS shall be developed in a general framework so that it can be easily expandable to address different networks, yet fast to compute.

In this study we describe both the main requirements of the proposed energy management system and its mathematical model. The novelties of this paper rely on the specific

This research was funded by the Research Fund for the Italian Electrical System under the Contract Agreement "Accordo di Programma 2019-2021 – PTR_19_21_ENEA_PRG_10" between ENEA and the Ministry of Economic Development.

978-1-6654-3613-7/21/$31.00 ©2021 IEEE

requirements, needs and general modular framework aimed to the future integration of the EMS with commercial software for AC/DC networks.

II. Functional Requirements of the Methodology

In this section we describe the functional requirements of the methodology proposed to successfully model generalized AC/DC networks, to be interfaced with external optimization power systems simulation tools, such as NEPLAN and PowerFactory.

A. General requirements

The main general functional requirements requested for the proposed methodology are as follows.

a) Easy to use and to be interfaced with other tools. The optimization tool shall be easy to use and simple to be interconnected with other external tools.

b) Flexibility to incorporate multiple components and types of components. General power systems networks can be composed by multiple components. General tools shall be able to address the main typologies of components, yet being able to be easily expanded depending on the specific needs of the user.

c) Flexible in accomodating different network configurations. General optimization tools shall account for the diversified nature of the power systems both in terms of number of components, their type and how they are connected.

d) Convergence towards the global optimal solution. The optimization tool shall guarantee the convergence of the optimization strategy towards the global optimum of the model representing the physical problem.

e) Fast to solve. Speed is a critical element for the operation of the system, as operators need to verify and act fast when changes in the available renewable energy, load and network asset occur.

These general requirements can guide the development of further methodologies to interface existing software with innovative optimization methodologies.

B. The need for an abstract model representation

The proposed optimization strategy shall be applied to general AC/DC networks, whose capacity and topology may be very diversified. Therefore, the methodology shall provide an abstract structure for describing general networks, where each physical component of the network is represented by a stereotyped abstract component. However, the formulation shall be simple to avoid a large growth in the problem complexity.

Similarly to the topology, the network components can be very different, with specific properties; however, from an energy point of view, common characteristics can be derived to classify the components based on their more relevant energy characteristics. For this reason, not only the network but also the components are proposed to be classified as abstract components.

III. The Abstract Optimization Methodology

A. From the physical to the abstract network model

In order to accomplish the functional requirements stated in the previous section, we propose a generalized methodology to derive the abstract network model, based on the physical components. The main procedure is composed as follows:

1) Identify the main characteristics of the components in terms of:

a) energy flows: direction, losses, among others;

b) characteristic functions: integral for storages, cost penalties when applicable, power/energy constraints, net power balance for busbars, etc.

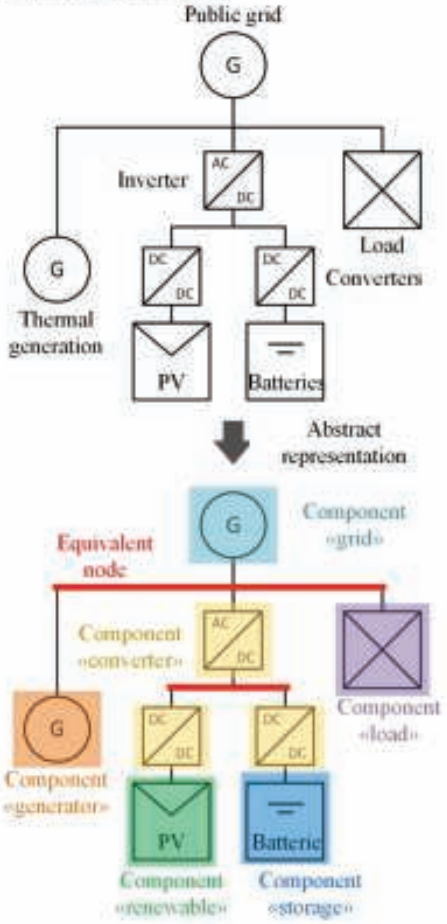

Fig. 1. Structure of a sample system

2) Focus on the main energy-related characteristics: drop the components characteristics that lead to secondary effects in terms of energy outcome, to handle the complexity.

3) Identify common characteristics among the components under consideration, e.g. loss function, storage dynamics, number of nodes, etc.

4) Group the characteristics to identify the abstract components: define a set of abstract components that capture and generalize the commonnalities among the selected physical components.

B. The software implementation

The most appropriate software implementation shall emerge from a compromise between (1) the complexity in the development of the optimization and (2) the available interfaces with the software expected to be used conjointly with the EMS. Based on the state-of-the-art, mathematical programming may be recommended for the development of EMS, given the ability to converge towards global optimization, such as in MILP methodologies or convex non-linear approaches [21]. However, the description of physical problem into mathematical can be sometimes very complex. Consequently, modelling algebraic frameworks to ease the description of the constraints and equations of the optimization models is recommended, as they enable describing the problem by explicitly listing them with algebraic symbols and simple mathematical operations. In this regard, many modelling languages, such as MATLAB [22], Python [23] or Julia [24] among others, can be chosen and the preference among them shall also account for complexity in the coding, execution speed and interfaces with external tools.

Main commercial tools (e.g. NEPLAN and PowerFactory) have developed interfaces for the Python code, which is a well-established open source software with many libraries and optimization tools. In particular, the Python-based modelling framework Pyomo [25] enables developers to easily customize optimization methodologies, also giving flexibility and modularity to the code. Moreover, the solver used to solve the problem can also be changed by the user depending on the license availability.

For these reasons, in this study we decided to represent the proposed abstract methodology in Python, using the Pyomo library.

IV. THE ABSTRACT ENERGY MANAGEMENT SYSTEM (EMS)

A. The software structure

The proposed abstract EMS is composed by a flexible core that converts the configuration files, loaded externally, into the proposed mathematical problem, as shown in Fig. 2. This formulation is powerful since there is no need to change the main optimization process for addressing a different system, in agreement with the functional requirements previously described and the goals of the project.

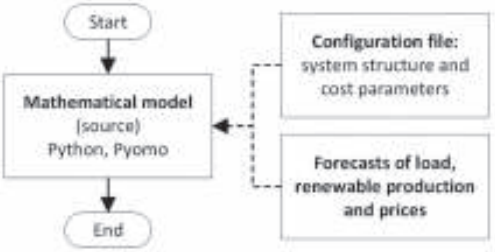

Fig. 2. Abstract EMS optimization process

B. The components

The first focus of the proposed EMS is the optimization and management of decentralized renewable sources and storage. Therefore, the following specific abstract components have been defined and implemented:

1) Component "grid": this component enables modelling the interconnection of the portion of the local system to the public grid. It is characterised by power limits and the energy exchange leads to economic costs or profits. Each instance of this component can be added to only a busbar. Any independent network shall have only a "grid" component to model a unique connection point, as typically done.

2) Component "battery": this component is aimed at modelling storage assets and in particular electrochemical batteries, which are very common devices in decentralised networks. Energy limits are accounted for as well as economic penalisation are considered to model the BESS wearing with its use. Similarly to the component grid, each asset of this component can be added to only a busbar.

3) Component "converter": this component type enables modelling energy losses due to the energy exchange between any two busbars. Power limits are considered and specialised depending on the energy flow.

4) Component "renewable": this component type enables modelling any non-dispatchable renewable generation asset, such as PV units of wind turbines. The power limits with respect to the available energy production are accounted for.

5) Component "load": this last component type enables modelling a load unit. This unit block accounts for reliability issues as it assures that the load shall be supplied at any time step, otherwise an economic penalty is added to the objective function.

C. Mathematical modelling

The main mathematical modelling of the abstract EMS is detailed in this section.

a) Objective function: the objective function to be minimized, shown in (1), accounts for the expected operating profit (OP), accounting for the net expenses ($\Delta GRID_t$) with respect to the public grid, the peak costs (C_t^{peak}), the costs (ΔC_t^{LC}) due to the energy not served and the wearing charges of the battery (ΔC_t^{wear}).

$$\max OP = \sum_{t\in T} \Delta GRID_t - C_t^{peak} - \Delta C_t^{LC} - \Delta C_t^{wear} \quad (1)$$

The net economic balance with respect to the grid is modelled in (2) proportionally to the power dispatch injected and withdrawn from any grid component g, where π_t^{sell} and π_t^{buy} are the selling and buying prices, and $P_{g,t}^{+}$ and $P_{g,t}^{-}$ represent the power injected (+) and withdrawn (-) from the public grid. The peak costs are described using (3)-(5). Equation (4) specifies that the peak costs occur proportionally to the power withdrawn from the public grid exceeds a given fraction and the economic cost is proportional to the exceeding power. Equation (5) guarantees that this cost is non-negative, whereas equation (3) enables accounting for networks having multiple independent connection points. Equation (6) describes the costs due to the load curtailment, which are proportional to the economic penalty c_l^{LC} for every type load component l. Finally, the wearing costs of the BESS are denoted in (7) as the sum over each battery-type components b of the product between the energy exchange with the battery and the economic penalty c_b^{wear}.

$$GRID_t = \sum_{g\in G} \pi_t^{sell} P_{g,t}^{+} - \pi_t^{buy} P_{g,t}^{-} \quad (2)$$

$$C_t^{peak} \geq \sum_{g \in G} C_{g,t}^{peak} \quad (3)$$

$$C_{g,t}^{peak} \geq c_g^{peak}\left(\max\left[P_{g,t}^{+}; P_{g,t}^{-}\right] - \beta_g^{peak}\right) \quad (4)$$

$$C_{g,t}^{peak} \geq 0 \quad (5)$$

$$C_t^{LC} = \sum_{l \in L} c_l^{LC} P_{l,t}^{LC} \quad (6)$$

$$C_t^{wear} = \sum_{b \in B} c_b^{wear}\left(P_{b,t}^{+} + P_{b,t}^{-}\right) \quad (7)$$

b) Component grid: the constraints for the grid components are the maximum power exchanges with respect to the public grid, as specified in (8). Equation (9) expresses the physical power dispatch at a generic node i, accounting for the proposed two variable representation.

$$0 \leq P_{g,\rightarrow i,t}^{+/-} \leq P_g^{size,+/-} \quad (8)$$

$$P_{g,\rightarrow i,t} = -P_{g,\rightarrow i,t}^{+} + P_{g,\rightarrow i,t}^{-} \quad (9)$$

c) Component battery: the battery component is characterised by both power and energy constraints, detailed in (10)-(14). Equation (10) guarantees the maximum nominal power of the BESS, whereas the constraint specifies that the charging (-) and discharging (+) process cannot occur in the same time step, where $P_{b,\rightarrow i,t}^{+/-}$ denotes the power dispatch of the battey. The energy balance within the battery is guaranteed by (13), where η_b is the battery efficiency and Δ is the time-step resolution. Finally, constraint (14) specifies that the energy stored in the battery shall lay between the maximum (α_b^{max}) and minimum (α_b^{min}) SOC of the battery. Equation (15) specifies the physical power dispatch at the generic node i, accounting for the proposed two variable representation of the battery.

$$0 \leq P_{b,\rightarrow i,t}^{+/-} \leq P_b^{size} \quad (10)$$

$$0 \leq P_{b,\rightarrow i,t}^{+} \leq z_{b,\rightarrow i,t} M_b \quad (11)$$

$$0 \leq P_{b,\rightarrow i,t}^{+} \leq \left(1 - z_{b,\rightarrow i,t}\right) M_b \quad (12)$$

$$E_{b,i\rightarrow j,t} = E_{b,\rightarrow i,t-1} + \Delta P_{b,\rightarrow i,t}^{-} \eta_b - \Delta \frac{P_{b,\rightarrow i,t}^{+}}{\eta_b} \quad (13)$$

$$\alpha_b^{min} E_b^{size} \leq E_{b,\rightarrow i,t} \leq \alpha_b^{max} E_b^{size} \quad (14)$$

$$P_{b,\rightarrow i,t} = -P_{b,\rightarrow i,t}^{+} + P_{b,\rightarrow i,t}^{-} \quad (15)$$

d) Component converter: the converter component enables the energy flow between any two different nodes i and j (16) and each component instance is characterized by two main variables $P_{c,i\rightarrow j,t}^{+/-}$, where (+) is non-null when the power physically flows from i to j, otherwise the other variable (-) is non-null. The power constraints are specified in (16)-(18): equation 16 states that the power flow cannot exceed the nominal capacity P_c^{size} and constraints (17) and (18) guarantee that the variables cannot be non-null in the same time step. Equation (19) and (20) finally specify the physical power dispatch occurring at the nodes i and j due to the converter connected between i and j.

$$0 \leq P_{c,i\rightarrow j,t}^{+/-} \leq P_c^{size} \quad (16)$$

$$0 \leq P_{c,i\rightarrow j,t}^{+} \leq z_{c,i\rightarrow j,t} M_c \quad (17)$$

$$0 \leq P_{c,i\rightarrow j,t}^{+} \leq \left(1 - z_{c,i\rightarrow j,t}\right) M_c \quad (18)$$

$$P_{c,\rightarrow i,t} = -P_{c,i\rightarrow j,t}^{+} + P_{c,i\rightarrow j,t}^{-} \quad (19)$$

$$P_{c,\rightarrow j,t} = P_{c,i\rightarrow j,t}^{+} \eta_c - \frac{P_{c,i\rightarrow j,t}^{-}}{\eta_c} \quad (20)$$

It is worth noticing that this generic type converter can be used to model any transmission component whose loss function can be approximated as a linear function. For the purpose of this study, we consider a linear efficiency model for both electronic components and transmission assets.

e) Component renewable: a generic renewable component is then described with equation (21), where $P_{r,\rightarrow i,t}^{+}$ represents the power dispatch of the renewable esset under consideration. P_r^{size} denotes the nominal capacity of the asset and $p_{r,t}^{av}$ is the specific renewable production for a time step t.

$$0 \leq P_{r,\rightarrow i,t}^{+} \leq p_{r,t}^{av} P_r^{size} \quad (21)$$

f) Component load: the model of a component load l connected to the bus i is described in (22)-(23), where (22) specifies that the power injected ($P_{l,\rightarrow i,t}$) to the busbar i. Note that the value is negative because the power is absorbed. Constraint (23) specifies that demand can be curtailed but up to the limit of the available load ($P_{l,t}^{L}$).

$$P_{l,\rightarrow i,t} = -P_{l,t}^{L} + P_{l,t}^{LC} \quad (22)$$

$$0 \leq P_{l,t}^{LC} \leq P_{l,t}^{L} \quad (23)$$

g) Busbar balance: finally, the power balance at each busbar i is implemented using (24), where A_i is the set of the assets connected to node i, and $P_{a,\rightarrow i,t}$ is the physical power exchanged at node i.

$$\sum_{a \in A_i} P_{a,\rightarrow i,t} = 0 \quad (24)$$

V. Case Study

The proposed methodology has been developed and tested on a case study of a microgrid system for a tramway station located in the northern part of Italy. Real demand has been used [26] and realistic renewable production data have been derived from [27]. The load profile of the tram has been properly measured for a day in April 2014 and adapted to 15-min time resolution. A constant demand of 1 kW is considered to supply auxiliary devices including security and lighting. The topology and design of the proposed system is shown in Fig. 3.

The buying and selling prices are chosen equal to 180€/MWh and 50€/MWh, respectively [28]. The roundtrip

efficiency of batteries is considered equal to 96%, the battery being operated between 90% and 10% SOC. Transformer efficiency is assumed to be 98%. Peak power costs are about 2.5 €/kW when exceeding the base power of 80 kW, which is assumed to be the standard peak typically paid for the considered day of the month [29].

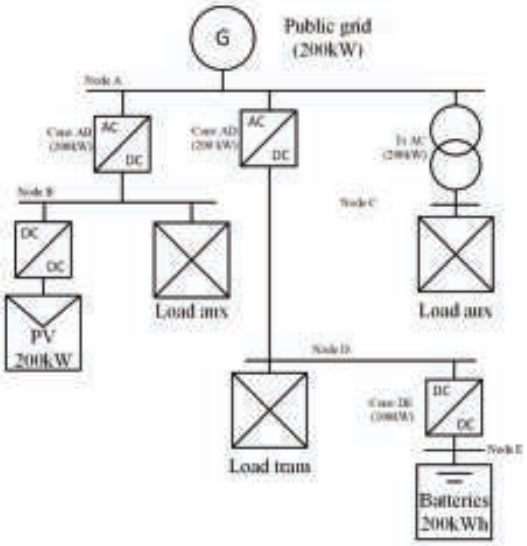

Fig. 3. Topology and characteristics of the case study.

VI. RESULTS

The main results of the proposed methodology are shown in Fig. 4 and Fig. 5. The methodology required a few seconds to be solved on an i7 core computer with 16Gb RAM, thus confirming its possible use for practical applications.

The total expected operating cost for the 1-day optimization is about 112 €: 0.14 € due to the battery wearing and 111.9 € is the net economic balance due to the public electricity market. Interestingly, thanks to the energy shifting enabled by the proposed optimization methodology, the peak power cost of 80 kW is guaranteed, thus no additional peak costs occur.

Fig. 4 clarifies that the demand is fully met without any curtailing, while losses in transformers, converters and battery system account for only 3% of it. Furthermore, the proposed scheduling methodology efficiently dispatches the PV system, and no renewable curtailment occurs. Therefore, the methodology enables achieving about 45% self-consumption, which goes in favor of the environmental goals and economics of microgrid management.

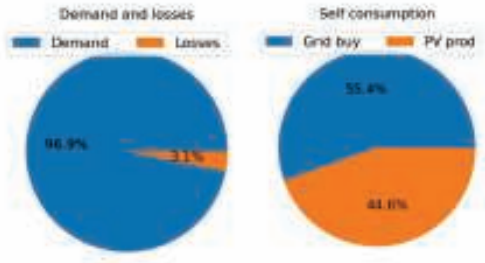

Fig. 4. Demand, losses and self-consumption.

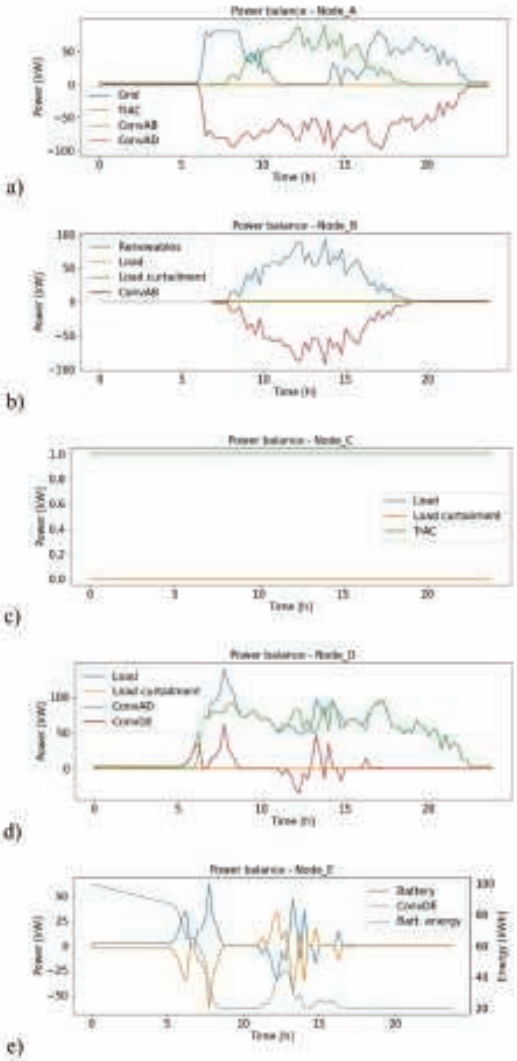

Fig. 5. Power balance at nodes A-E.

To further clarify how the proposed EMS operates, Fig. 5 shows the power and energy balance at each busbar of the microgrid under consideration. In particular, Fig. 5(a) clarifies that the power dispatch with the grid does not go beyond 80 kW. Therefore, the demand located at nodes B, C and E is only partially met with the energy bought from the grid. In the first hours of the day (6-8am), the renewable production is not able to provide adequate production, as shown by the green power profile in Fig. 5(a) that is the power supplied by the converter "Conv AB" that enables the power flow between the DC node B, where the PV plant is tied, and node A. The largest power flow in the microgrid occurs through converter "Conv AD" because the DC node D is the one supplying the tram. In particular, the tram demand is met both through "Conv AD" and "Conv DE". Since the batteries are tied at the bus E, the power flow between D and E is bidirectional and the battery

charging occur during daytime, when the PV production is abundant. This confirms the suitability of the proposed tool for managing mixed AC-DC networks, which are expected in the near future.

VII. Conclusions

This paper reports the development of a flexible Python tool for the optimal operation of a microgrid including mixed AC/DC networks. The proposed methodology has proven to be robust, fast and accurate in finding the optimal scheduling of a mixed AC/DC system for tram transport applications. The described Energy Management System is flexible and proven to be able to successfully be used conjointly with established commercial tools, such as NEPLAN and PowerFactory.

This suggest that the tool discussed in this paper can be used in practical applications and lay the foundation for addressing the operation of even more complex AC/DC networks.

References

[1] E. Panos and M. Densing, "The future developments of the electricity prices in view of the implementation of the Paris Agreements: Will the current trends prevail, or a reversal is ahead?," *Energy Econ.*, vol. 84, p. 104476, 2019, doi: 10.1016/j.eneco.2019.104476.

[2] L. Fiorini, G. A. Pagani, P. Pelacchi, D. Poli, and M. Aiello, "Sizing and Siting of Large-Scale Batteries in Transmission Grids to Optimize the Use of Renewables," *IEEE J. Emerg. Sel. Top. Circuits Syst.*, vol. 7, no. 2, pp. 285–294, 2017, doi: 10.1109/JETCAS.2017.2657795.

[3] A. Baccioli, L. Ferrari, F. Vizza, and U. Desideri, "Potential energy recovery by integrating an ORC in a biogas plant," *Appl. Energy*, vol. 256, 2019, doi: 10.1016/j.apenergy.2019.113960.

[4] J. Lowitzsch, C. E. Hoicka, and F. J. van Tulder, "Renewable energy communities under the 2019 European Clean Energy Package – Governance model for the energy clusters of the future?," *Renew. Sustain. Energy Rev.*, vol. 122, p. 109489, Apr. 2020, doi: 10.1016/j.rser.2019.109489.

[5] European Parliament, "Directive 2019/944 on Common Rules for the Internal Market for Electricity," *Off. J. Eur. Union*, no. L 158, p. 18, 2019, [Online]. Available: http://www.omel.es/en/files/directive_celex_32019l0944_en.pdf.

[6] S. Kakran and S. Chanana, "Smart operations of smart grids integrated with distributed generation: A review," *Renew. Sustain. Energy Rev.*, vol. 81, pp. 524–535, Jan. 2018, doi: 10.1016/j.rser.2017.07.045.

[7] C. Wang, Y. Liu, X. Li, L. Guo, L. Qiao, and H. Lu, "Energy management system for stand-alone diesel-wind-biomass microgrid with energy storage system," *Energy*, vol. 97, pp. 90–104, 2016, doi: 10.1016/j.energy.2015.12.099.

[8] R. Palma-Behnke, C. Benavides, F. Lanas, B. Severino, L. Reyes, J. Llanos, and D. Saez, "A microgrid energy management system based on the rolling horizon strategy," *IEEE Trans. Smart Grid*, vol. 4, no. 2, pp. 996–1006, 2013, doi: 10.1109/TSG.2012.2231440.

[9] M. H. Oboudi, R.-A. Hooshmand, and S. Rahimi, "Stochastic Operation Framework of Microgrid under Uncertainties of Load, Generation, and Contingency," *J. Energy Eng.*, vol. 146, no. 1, 2020, doi: 10.1061/(asce)ey.1943-7897.0000639.

[10] L. Bartolucci, S. Cordiner, V. Mulone, and J. L. Rossi, "Hybrid renewable energy systems for household ancillary services," *Int. J. Electr. Power Energy Syst.*, vol. 107, pp. 282–297, May 2019, doi: 10.1016/j.ijepes.2018.11.021.

[11] L. Bartolucci, S. Cordiner, V. Mulone, V. Rocco, and J. L. Rossi, "Renewable source penetration and microgrids: Effects of MILP – Based control strategies," *Energy*, vol. 152, pp. 416–426, 2018, doi: 10.1016/j.energy.2018.03.145.

[12] Y. Jia, P. Wen, Y. Yan, and L. Huo, "Joint operation and transaction mode of rural multi microgrid and distribution network," *IEEE Access*, vol. 9, pp. 1–1, 2021, doi: 10.1109/access.2021.3050793.

[13] J. J. Justo, F. Mwasilu, J. Lee, and J. W. Jung, "AC-microgrids versus DC-microgrids with distributed energy resources: A review," *Renew. Sustain. Energy Rev.*, vol. 24, pp. 387–405, 2013, doi: 10.1016/j.rser.2013.03.067.

[14] S. M. Bagher Sadati, J. Moshtagh, M. Shafie-khah, A. Rastgou, and J. P. S. Catalão, "Operational scheduling of a smart distribution system considering electric vehicles parking lot: A bi-level approach," *Int J Electr. Power Energy Syst.*, vol. 105, 2019, doi: 10.1016/j.ijepes.2018.08.021.

[15] A. Ahmad Khan, M. Naeem, M. Iqbal, S. Qaisar, and A. Anpalagan, "A compendium of optimization objectives, constraints, tools and algorithms for energy management in microgrids," *Renew. Sustain. Energy Rev.*, vol. 58, pp. 1664–1683, 2016, doi: 10.1016/j.rser.2015.12.259.

[16] O. O. Amusat, P. R. Shearing, and E. S. Fraga, "Optimal design of hybrid energy systems incorporating stochastic renewable resources fluctuations," *J. Energy Storage*, vol. 15, pp. 379–399, 2018, doi: 10.1016/j.est.2017.12.003.

[17] M. Giumoli, P. Pelacchi, and D. Poli, "On the use of simplified reactive power flow equations for purposes of fast reliability assessment," *IEEE EuroCon 2013*, no. July, pp. 992–997, 2013, doi: 10.1109/EUROCON.2013.6625102.

[18] D. Fioriti and D. Poli, "A novel stochastic method to dispatch microgrids using Monte Carlo scenarios," *Electr. Power Syst. Res.*, vol. 175, no. October 2019, 2019, doi: 10.1016/j.epsr.2019.105896.

[19] NEPLAN, "NEPLAN," 2021. https://www.neplan.ch/.

[20] DigSilent, "PowerFactory," 2021, [Online]. Available: https://www.digsilent.de/en/powerfactory.html.

[21] S. Boyd and L. Vandenberghe, *Convex Optimization*. 2004.

[22] MathWorks, "MATLAB," *MathWorks*, 2021. https://it.mathworks.com/.

[23] Python, "Python," 2021. https://www.python.org/.

[24] Julia, "Julia," 2021. https://julialang.org/.

[25] Pyomo, "Pyomo - Python," 2021. https://pyomo.readthedocs.io/en/stable/index.html.

[26] M. Ceraolo, R. Giglioli, G. Lutzemberger, and A. Bechini, "Cost effective storage for energy saving in feeding systems of tramways," in *2014 IEEE International Electric Vehicle Conference (IEVC)*, 2015, pp. 1–6, doi: 10.1109/IEVC.2014.7056112.

[27] S. Pfenninger and I. Staffell, "Renewables.ninja platform," 2020. https://www.renewables.ninja/.

[28] ARERA, "Obiettivi Strategici e linee di intervento 2019-2021: Area Energia," *2020*. .

[29] S. Barsali, R. Giglioli, M. Giantoli, G. Lutzemberger, and D. Poli, "Control strategies and real time operation of storage systems integrated with MV photovoltaic plants," in *Int. Conf. on Env. and Elect. Engineering, EEEIC*, 2015, pp. 243–248, doi: 10.1109/EEEIC.2015.7165546.

3.7 Bidirectional Solid-State Circuit Breakers for DC Microgrid Applications

Bidirectional Solid-State Circuit Breakers for DC Microgrid Applications

Ivan Navoni
dept. of Energy
Politecnico di Milano
Milano, Italy

Michela Longo
dept. of Energy
Politecnico di Milano
Milano, Italy
michela.longo@polimi.it

Morris Brenna
dept. of Energy
Politecnico di Milano
Milano, Italy
morris.brenna@polimi.it

***Abstract*—The aim of this work is to investigate on DC microgrids and to find all the advantages and disadvantages of this type of configuration, in particular to find a solution for the problem of protection devices. In this paper, different types of circuit breaker devices are analyzed in order to find a possible solution to the main criticality of this distribution system. Two different configuration of Solid-State Circuit Breaker (SSCB) are analyzed and simulated in a DC microgrid using Simulink/Matlab.**

Keywords*— *DC Microgrid, Distributed Generation, SSCB, Fault analysis, Protection devices.

I. INTRODUCTION

Microgrid is a small distribution network that can be connected to the main grid or can be autonomous depending on the operating mode [1, 2]. Generally, microgrids have two operating mode: normal and islanding modes. During the normal operations the microgrid is connected to the main grid at point of common coupling, in which the voltage levels are synchronized and kept at the same magnitude. Microgrids go into islanding mode when a disturbance happens in the main grid. In islanding mode, they can be self-supplied thanks to the Distributed Generation (DG) like fuel cell, wind turbine, and photovoltaic array [3-5]. Nowadays, with the increase of DG, DC load and vehicle charging station the interest on DC microgrids instead of traditional AC has increased in order to improve the efficiency. On the other hand, DC microgrid have some problems, the main problem is about protection strategies and protection devices [6-9]. In this paper, the DC microgrids are analyzed, with a particular focus in the advantages and disadvantages of DC microgrids. Then, an analysis about different possible protection devices is carried out and then the different solutions are compared in order to present all the advantages and disadvantages of the different types. Two different configurations of solid-state circuit breaker are analyzed and simulated in a DC microgrid using Simulink/Matlab.

II. GENERAL CONSIDERATIONS

Two different types of Solid-State Circuit Breakers (SSCB) are chosen the simulation and the comparison between these different solutions are explained in this section. It is important during the comparison to take in consideration that each topology is design for the same condition of operation [10, 11]. For these simulations the data sheets of real electronic components are used to make sure that all the configurations could be done and that are realizable. Obviously, the same components are used for the breakers in order to make the comparison more interesting and so even the time delay and all the other physical limits of the component are the same for the two different configurations [12].

Research Fund for the Italian Electrical System under the Contract Agreement between ENEA and the Ministry of Economic Development.

978-1-6654-3613-7/21/$31.00 ©2021 IEEE

The two different topologies of DC circuit breaker are proved in a simple circuit, only with elementary component, and then so the correct behavior of these type of configuration is proved. Once this first step is done, then these circuit breaker solutions will be tested on a complex DC microgrid with the use of PV and battery [13-15].

The two different solutions tested are two SSCB breakers with different clamping circuit. This circuit is used to reduce the voltage across the power electronic component during the interrupting operation [16]. Since without this type of circuit the voltage will be too high for the electronic component, and it will collapse and break. The configurations under analysis are respectively the RDC configuration, where the capacitor is charged and discharged during the breaking simulation, and the MOV configuration that used a metal oxide varistor in order to keep the voltage within the maximum limits of the electronic component. The choice of IGBT is done in relation to advantages and disadvantages of this electronic component. The main advantages of IGBT are:

- The low on-state voltage drops and high forward conduction current density. Thus, due to very low on-state voltage drop caused by the conductivity modulation and the high forward conduction density compared to the MOSFET and bipolar transistor, it is possible to use a smaller chip and so to reduce costs.
- Low driving power and a simple drive circuit due to the input MOS gate structure. Thus, the IGBT can be controlled in an easier way compared to current controlled devices (thyristor, BJT) in high voltage and high current applications.
- Wide SOA: With respect to output characteristics, the IGBT has superior current conduction capability compared with the bipolar transistor. It has also an excellent forward and reverse blocking capabilities.

The main disadvantages are:

- The switching speed is slower compared to that of the power MOSFETs, but it is superior to that of the BJT. The collector current tailing due to the minority carrier causes the turn-off speed to be slow but this speed is still faster than that of circuit breaker.
- There is the possibility of latch-up due to the internal because it is the PNPN thyristor structure.

Anyway, these disadvantages do not affect the required characteristic of the SSCB in this configuration. Thus, with these advantages the IGBT is selected. The DC voltage level used to carry on the simulation is 400V for both the circuit breakers for both the first type of simulations and 1500V for the simulation in the complex LVDC. So, the choice of the IGBT and of the other components such as MOV, Cs, RS is based on the system configuration al levels, but the choice of

these auxiliary component will be discussed in further sections. All the comparison will be done considering the total breaking time, the size of the components, the maximum current in the line and the energy dissipated in the breaking process.

III. Circuit Breaker Models

The first type of circuit breaker used is a Solid-State Circuit Breaker with an RDC snubber circuit as shown in Fig. 1, namely a circuit in parallel to the breaker made of a resistor, a capacitor, and a diode. The capacitor is essential for the reduction of the voltage across the power electronic device and so of the power losses during the turn-off of the breaker. The resistor is used for the discharge of the capacitor after the trip of the breaker, and it is also fundamental for the reduction of the peak value of the current during turn off and turn on operations.

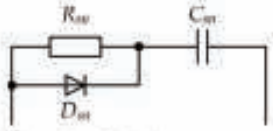

Fig. 1. RDC SSCB network configuration.

The presence of this snubber avoids a high value of *di/dt* that could produce a high voltage during the transient resulting on a failure of the SSCB. Thus, this component is used to stay within the limit of safety operation of the electronic component such as IGBT in this case, and so ensure the correct operation of the breaker. So, one of the most important consideration for the snubber is the correct selection of the component, and this choice is based on the behavior of the snubber circuit. This interruption method has three different stages as shown in Fig. 2.

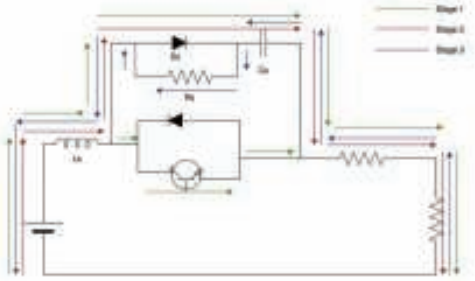

Fig. 2. Snubber process: Stage 1, Stage 2 and Stage 3.

In Stage 1, the current commutates from the solid-state circuit breaker to the snubber circuit trough the diode and the capacitor. In Stage 2, the capacitor C_S get charged until it reaches the maximum voltage value. Stage 3 represents the moment when the capacitor discharge trough the resistor R_S. After the snubber circuit turns on the bus current continue to increase its value, and during this rise of the current the current suppression of the bus is weakened by the C_S, so the presence of the snubber increases the peak value of the current compared to the simple circuit without the presence of the RCD snubber. During Stage 1(from 0 to t_f), the diode D_s is turned on and the bus current start to commute from the SSCB path to the snubber circuit as shown in Fig. 2. Before this there is a delay when the current in the solid-state circuit breaker increase due to the gate driver that reveals a high current and decide to turn-off the breaker. At t_f the snubber current is equal to the bus current and the current in the SSCB becomes zero, so the IGBT is completely reversed block, and this coincide with the end of Stage 1. At the end of this stage the current and voltage are considered as shown in Eq. (1):

$$\begin{cases} ic_s(tf) = I_{bus} \\ uc_s(tf) = 0 \end{cases} \tag{1}$$

During Stage 2, the capacitor C_s start charging trough D_s as shown in Fig. 2. This step ends when the fault energy that was stored in the stray inductance is totally given to the capacitor (Eq. (2)).

$$\begin{cases} i_{bus}(tr1) = 0 \\ uc_s(tr1) = U_{RR} \\ t_{r1} = \dfrac{1}{\omega_1} arctan \dfrac{\omega_1}{\alpha_1} - \dfrac{\beta_1}{w_1} + t_f \end{cases} \tag{2}$$

The design of the parameters of RCD snubbers, is based on the following circuit parameters: equivalent bus inductance L_s; equivalent bus resistor R; de-link voltage u_{DC}; rated bus current I_r; the delay time t_h; the turn-off time for IGBT t_f; the shortest time for SSCB reclosure $T_{reclose}$; the peak current through IGBTs allowed at SSCB reclosure I_{max}; the junction capacitance C_J; the maximum voltage allowed for SSCB is U_{max}. As SSCBs on positive and negative buses share u_{DC} equally when they reach the steady state, the reference voltage for u_{SSCB} is set as u_{DC} (1.0 p.u.). There are some different techniques for designing a snubber, one of those is the following. The first step to do is to determinate the bus current before the turn on of the snubber and it can be derived as identified in Eq. (3):

$$I_{bus} = -\left(\frac{u_{DC}}{R} - I_r\right) e^{-\frac{R}{L_S} t_h} + \frac{u_{DC}}{R} \tag{3}$$

The second step consist in the calculation of the snubber capacitance based on the energy conservation law with energy exhaustion on R neglected using Eq. (4):

$$\begin{cases} \frac{1}{2} C_{S0} \left(U^2_{max} - u^2_{CS}(0) \right) = \frac{1}{2} L_s \left(I^2_{bus} - i^2_{bus}(t_r) \right) \\ C_S = \alpha_C C_{S0} \end{cases} \tag{4}$$

In which $u^2_{CS}(0) = 0$ and $i^2_{bus}(t_r) = 0$, and α_C is a parameter that should first be chosen close to 1 according to real capacitance values, and then could be increased if the maximum overvoltage exceeds the limits. The third step is related to the choice of R_s. The lower limit for snubber resistance R_{Smin} can be determined by calculating the peak current at SSCB reclosure as reported in Eq. (5):

$$\begin{cases} I_m = \dfrac{u_{DC}}{2R_{Smin}} \\ R_S = \alpha_R \dfrac{u_{DC}}{2I_m} \end{cases} \tag{5}$$

The coefficient α_R should first be chosen close to 1 in the same way as α_C, and then it has to be increased if the overcurrent exceeds the limits.

IV. DC IDEAL NETWORK SIMULATION

The first simulation is carried out in a simplified and ideal DC network in order to see the behaviors of the different types of circuit breaker. The simplified network has a voltage of 400V with a R-L load. In this network the stray inductance indicated with L_s has a value of some mH to simulate the internal inductance of the generator. This inductance is the element that has the energy stored during the steady state and that has to dissipated during a fault or an opening condition. In this case L_s= 10 mH. This first simulation is carried out in a simple DC network in order to understand the behavior of the devices and to ensure the correct application for these type of circuit breakers. The first DC circuit breaker configuration is shown in Fig. 3. This configuration represents the RCD type, so the circuit breaker with a parallel branch made of a resistor a capacitor and a diode used to dissipate the energy and protect the electronic component. In both the configuration a gate drive circuit measure the current and if it exceeds a limit, it decides automatically to activate the circuit breaker and to open it. The correct choice of the snubber component is fundamental for the correct behavior of the SSCB, thus based on the previous considerations the components that have to be sized are C_s and R_s.

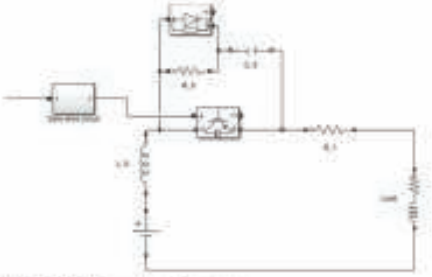

Fig. 3. RDC SSCB network configuration.

In this case the values of these parameters are $C_s = 400\ \mu F$ and $R_s = 10\ \Omega$. With this configuration the results of the trip of the circuit breaker with a line-to-line fault is shown in Fig. 4. As can be seen the sizing of the passive element can be considered corrected and the breaker is able to interrupt the current.The problem with this configuration is the overvoltage, since in fault condition the voltage reach a peak value higher than 900V, that is more than two times the voltage level. This overvoltage is applied to a capacitor of 400 μF, and so this element has to dissipate too much in this condition, and this higher voltage may cause short through the capacitor and burnup. For these reasons this configuration can only be used as a disconnector.

Figure 5 shows the behavior of the device in opening operation during normal condition and not in short circuit condition. As expected, the voltage peak across the circuit breaker in this condition is lower than in short circuit condition. This overvoltage lower than 500V is acceptable and so this device can be used correctly as a contactor. As can be seen in Fig. 5, the current in the device is instantaneously zero when the breaker opens, and the residual current flows through the snubber path and can be seen from the line current, that goes to zero causing a low overvoltage across the SSCB. When the transient finish the voltage across the SSCB reaches the network voltage level of 400V and the current reaches the zero. This end the opening process, and the total clearing time is $T_{clearing}$= 20ms. The total energy dissipated in the process from the circuit breaker is E_{diss}=84.4 J. As can be seen in Fig. 4 the current in the electronic device increases for the first nanoseconds, this is due to the time delay tb of the IGBT and to the gate drive circuit that have to detect the fault. However, the current reaches the value of 72A and in this case stay below the limit of the IGBT and so this is not dangerous for the device itself. The second configuration is shown in Fig. 6.

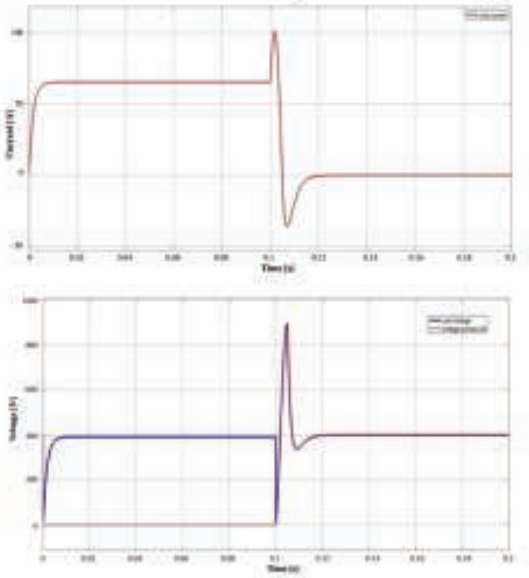

Fig. 4. Behavious of SSCB with RCD snubber in fault conditions (a) current and (b) voltage.

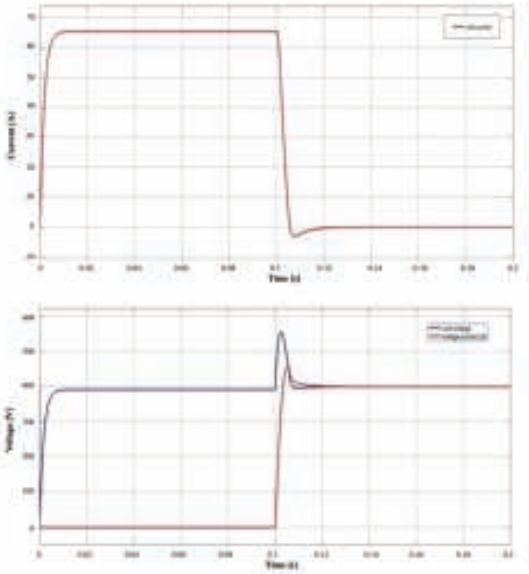

Fig. 5. Behavious of SSCB with RCD snubber working as a disconnector (a) current and (b) voltage.

This circuit breaker set up correspond to a double direction solid-state circuit breaker with a metal-oxide varistor

connected in parallel to the electronic component. The component, as said before, is used to avoid high overvoltage across the IGBT and dissipate the energy. It is either possible to use one MOV for both the IGBT's or to use to use two different MOV, since this component is bidirectional, and the fault current flow in one direction. The choice two MOV is done since the MOV has not a long lifetime due to the degradation during the process of energy absorption, for this reason, it is possible to choose two MOV and increase the life of the component in case of fault in different directions.

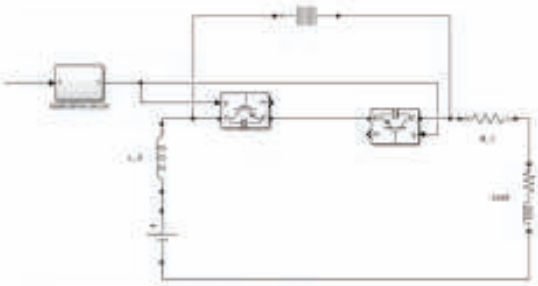

Fig. 6. MOV SSCB network configuration.

The behavior of this type of circuit breaker is shown in are shown in Fig. 7. As can be seen, as the gate drive circuit is the same as before and the component are sized correctly, the peak of the current is almost the same as in Fig. 4.

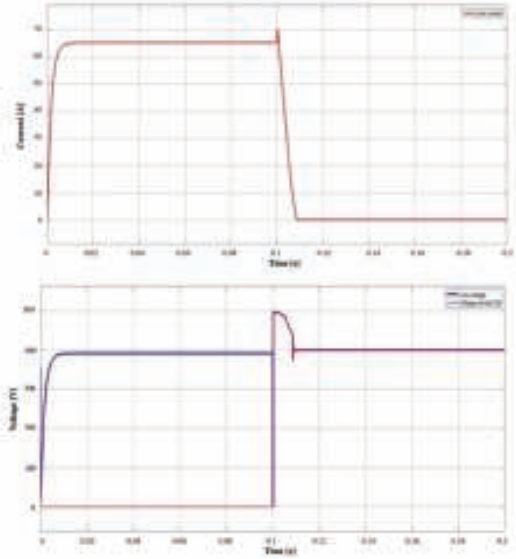

Fig. 7. Behavious of MOV SSCB in fault conditions (a) voltage and (b) current.

Thus, the current in the electronic component and in the line remains within the limits. In this condition due to the effect of the MOV the maximum peak voltage across the solid-state circuit breaker remains lower, and it reach only 500 V, that is a value acceptable for this configuration. Thus, differently from the RDC SSCB, this configuration can be adopted in case of short-circuit and so can be used as a proper circuit breaker. The current reaches the zero slower than with the RCD SSCB, but even in fault condition it ensure a lower voltage peak, that will not affect the network. The clearing time in this configuration id $T_{clearing}$=12 ms. The total energy dissipated in the process from the circuit breaker is E_{diss}=72 J. This reduction in dissipated energy is expected, since the clearing time is lower than in RCD SSCB.

V. DC Microgrid Configuration

The DC microgrid is a VSC-based LVDC transmission line of 2MVA at (+/-750V). The interconnection between the grid is made with a traditional three phase, two level VSC connected to the Low-Voltage AC grid with the interposition of a transformer. VSC is the main technology able to connect DC and AC networks, a grid connected VSC is responsible for the exchange of power between the AC and DC grids. The pulse signal comes from a control loop used to keep the voltage level constant at 1500V on the low voltage DC transmission line and control the bridge, in particular with the use of a PID regulator that controls the switching frequency of the converter in order to keep the output value constant. In these simulations the configuration used is a two-terminal structure, so with two converter satiations configurated as in Fig. 8, and the transmission line is powered from two different terminals.

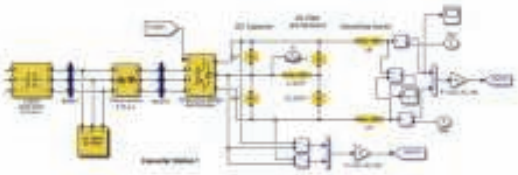

Fig. 8. SVC Converter station

Thus, in case of fault in a portion of the transmission line, or in case of disconnection of one feeder due to fault or maintenance the distribution network remains powered by the other feeder connected. The two elements connected to this VCS-Based low voltage DC microgrid are a PV array and a charging infrastructure, the first one injects power to the grid and so is considered as a generator, and the second one acts like a load. As done for the ideal network two different type of circuit breaker will be tested in the following simulations, and these SSCB are the RCD and the MOV circuit breaker. The design of the components used in these two types of configurations must be done. The sizing approach is the same as before for the two different conditions. In these simulation as seen in Fig. 9 the SSCB is a bipolar circuit breaker, it reduces the overvoltage across the single power semiconductor device and increase the safety, since if one of the SSCB trip fails, the other one can anyway interrupt the current.

Fig. 9. Complete simulink model.

The first type of circuit breaker configuration is shown in shown in Fig. 10. This circuit breaker has the same topology as the one shown in Fig. 3. The main difference is the bidirectionality of this SSCB, since the use of two electronic devices in opposite direction make it possible to the breaker to trip in both the directions. As seen previously the importance of the correct sizing of the passive elements is fundamental for a correct behavior of the circuit breaker. In this configuration the values for the components are $C_S = 10\ \mu F$ and $R_S = 10$ ohm. As seen in the simulation for the ideal DC network this component is simulated in case of normal operation, and it open at T=3.5s. The case of line-to-line fault is analyzed in Fig. 11.

Fig. 10. RCD SCCB configuration in low voltage transmission line.

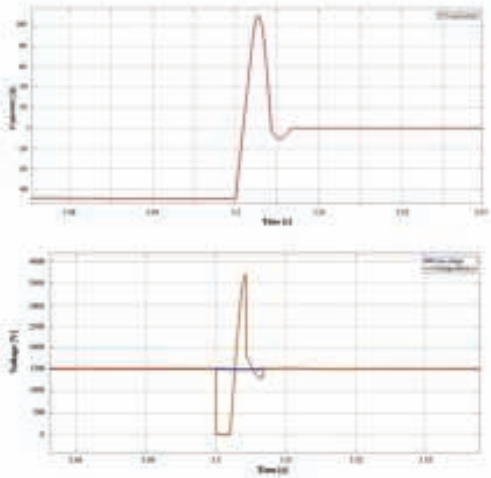

Fig. 11. Behaviuors of SCCB with RCD snubber in LVDC microgrid (a) current and (b) voltage.

In this case as can be seen there is an overvoltage in the line due to the operation of the solid-state circuit breaker. In particular, the voltage measured before the line inductance *Ls* drop to zero when the short circuit occurs and stay at this value until the gate drive system detect an over current and decide to trip the electronic component, this time is equal to 2ms. After this operation the real behavior of the circuit breaker can be analyzed. After this moment the voltage start to rise and the capacitor start the charging stage, and the current start to reduce its slope and to reduce until it reaches the zero and the voltage stabilize at 1500V, the line voltage level. The peak current value is 110 A, this value stays within the limit of the line, so the overcurrent does not affect the insulation of the cable. The total clearing time is $T_{clearing}$= 7 ms. In this network topology this configuration of SSCB cannot work as a circuit breaker, since in short-circuit conditions, the overvoltage reached in the derivative line before the inductance is too high and can damage the insulation of the cables and of the components, even if the current is interrupted in a short time. In the same way as founded in the simulation for an ideal DC network, this configuration can be used as a disconnector.

The second type of SSCB simulated is the solid-state circuit breaker with a MOV in parallel used to dissipate the energy stored during short circuit as seen in Fig. 12.

Fig. 12. MOV SCCB configuration in low voltage transmission line.

This circuit breaker has the same topology as the one shown in Fig. 6, in fact the MOV is in parallel to the IGBT, and when the electronic component is opened the MOV is in series with the line and can dissipate the energy created by the short-circuit. With this configuration of the SSCB the simulation of short-circuit are carried on, and the result can be seen in Fig. 13. As can be observed with this configuration the solid-state circuit breaker is able to interrupt the current in short-circuit conditions. In fact, the maximum overvoltage reached is 2000V that can be accepted by the cables and the element present in the derivative line. As can be seen there are some ripples in the voltage line level, but these ripples value is about 20V that with a voltage line level of 1500V is less than 2% and least for 20ms, so this oscillation will not affect the other element in the DC distribution line, and in the AC, line connected to the microgrid. The current is correctly interrupted before it reaches the short-circuit value, in fact it reaches 80A an then start to reduces, it means that the gate drive circuit is correct, and the value of the current stay within the limit of the line cables. The total clearing time of this configuration is $T_{clearing}$= 8ms.

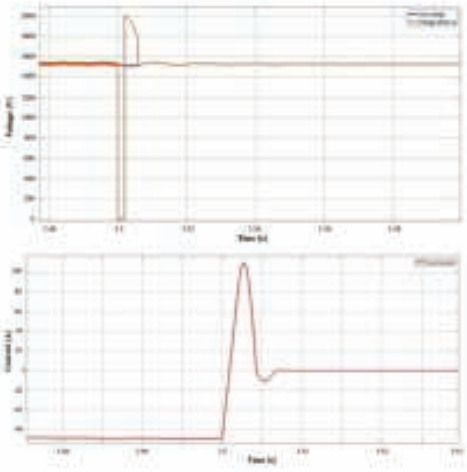

Fig. 13. Behaviours of MOV SCCB in LVDC microgrid (a) current and (b) voltage.

VI. CONCLUSIONS

The aim of this work is to investigate on DC microgrids and to find all the advantages and disadvantages of this type of configuration, in particular to find a solution for the problem of protection devices. In this paper, different type of circuit breaker devices is analyzed in order to find a possible solution to the main criticality of this distribution system.

Two types of solid-state circuit breaker with different voltage clamping circuit are studied. The SSCB with the linear voltage clamping solution use an RCD snubber circuit, when the capacitor absorbs some of the inductive energy stored in the line inductor, and the charging of the capacitor reduce the voltage rise rate and the peak value of voltage across the power semiconductor device. The resistor in series is used to avoid the oscillation of the snubber and reduce the discharge current into the power device. However, the presence of the resistance in the circuit increases the voltage drop and reflect it on the power semiconductor device. In fact, as seen in the simulations even if this configuration has a high speed and low switching losses the overvoltage could be a problem in some applications. This topology is the simplest and offers the lowest requirements in order of components and semiconductor devices. Another great problem is the sizing of the component and in particular of the capacitor, since this configuration need a high capacitor in the order of tens or hundreds of μF, and this element cannot bear high voltages without problems. Anyway, this configuration with some improvement can be used as a disconnector, and so open the circuit in normal condition, when the overvoltage caused by the process is lower. The SSCB with the non-linear clamping voltage solution use a metal-oxide varistor connected in parallel to the electronic device. This non-linear component can change its resistance value. During the circuit breaker turn-off process, when the clamping voltage is reached, the voltage across the MOV remains constant, with a progressive decrease in voltage as the inductive energy stored in system inductance is dissipated through this component. This magnetic energy stored in the circuit is greatly influenced by the system current and from the system inductance. The selection an appropriate MOV, with a safe clamping voltage is important for the power semiconductor device. This SSCB topology is a bit slower and has higher losses compared to the linear solution, but it allows to have lower overvoltage. However, the MOVs have not a long lifetime due to their degradation during the process of energy absorption.

This is a limit for the number of turn-off operations that can be done using MOVs. Another problem is that a MOV with a satisfying characteristic may not be found and the practical implementation in the real circuit breaker could be complicated. There are a lot of studies about low voltage DC circuit breakers technology in order to have more efficient and fast devices. Furthermore, to have more realistic models the stray components should be considered and some simulation and experimental tests with real component should be done in order to confirm the behavior of the configurations. There are other different methods to interrupt the current in this type of networks such as hybrid circuit breakers, and some investigation and simulation about this type of circuit breaker can be done. A possible solution for the improvement of non-linear voltage clamping circuit is the use of TVS.

ACKNOWLEDGMENT

This research was funded by the Research Fund for the Italian Electrical System under the Contract Agreement "Accordo di Programma 2019-2021 – PTR_19_21_ENEA_PRG_10" between ENEA and the Ministry of Economic Development.

REFERENCES

[1] G. L. de Andrade and T. P. de Leão, "A brief history of direct current in electrical power systems," 2012 Third IEEE HISTory of ELectro-technology CONference (HISTELCON), Pavia, 2012, pp. 1-6, doi: 10.1109/HISTELCON.2012.6487566.

[2] C. L. Sulzberger, "Triumph of AC - from Pearl Street to Niagara," in IEEE Power and Energy Magazine, vol. 1, no. 3, pp. 64-67, May-June 2003, doi:

[3] H. Lotfi and A. Khodaei, "AC Versus DC Microgrid Planning," in IEEE Transactions on Smart Grid, vol. 8, no. 1, pp. 296-304,

[4] J. Lago and M. L. Heldwein, "Operation and Control-Oriented Modeling of a Power Converter for Current Balancing and Stability Improvement of DC Active Distribution Networks," in IEEE Transactions on Power Electronics, vol. 26, no. 3, pp. 877-885, March 2011

[5] Y. Wang, W. Li, X. Wu and X. Wu, "A Novel Bidirectional Solid-State Circuit Breaker for DC Microgrid," in IEEE Transactions on Industrial Electronics, vol. 66, no. 7, pp. 5707-5714, July 2019, doi: 10.1109/TIE.2018.2878191.

[6] S. Lee and Hyosung-Kim, "A study on Low-Voltage DC circuit breakers," 2013 IEEE International Symposium on Industrial Electronics, Taipei, 2013, pp. 1-6, doi: 10.1109/ISIE.2013.6563723.

[7] Y. Du et al., "A high-reliability dc distribution network topology," 2017 IEEE Conference on Energy Internet and Energy System Integration (EI2), Beijing, 2017, pp. 1-5, doi: 10.1109/EI2.2017.8245619.

[8] J. Yang, J. E. Fletcher and J. O'Reilly, "Multiterminal DC Wind Farm Collection Grid Internal Fault Analysis and Protection Design," in IEEE Transactions on Power Delivery, vol. 25, no. 4, pp. 2308-2318, Oct. 2010, doi: 10.1109/TPWRD.2010.2044813.

[9] K. A. Prakash, A. Lallu, F. R. Islam, and K. A. Mamun, "Review of power system distribution network architecture," 2016 3rd Asia-Pacific World Congress on Computer Science and Engineering (APWC on CSE), pp. 124–130, 2016. R. Rodrigues, Y. Du, A. Antoniazzi and P. Cairoli, "A Review of Solid-State Circuit Breakers," in IEEE Transactions on Power Electronics, vol. 36, no. 1, pp. 364-377, Jan. 2021, doi: 10.1109/TPEL.2020.3003358.

[10] J. Millán, P. Godignon, X. Perpiñà, A. Pérez-Tomás and J. Rebollo, "A survey of wide bandgap power semiconductor devices", IEEE Trans. Power Electron., vol. 29, no. 5, pp. 2155-2163, May 2014.

[11] V. Victor, B. Steiner, K. Lawson, S. B. Bayne, D. Urciuoli and H. C. Ha, "Suitability of n-ON recessed implanted gate vertical-channel SiC JFETs for optically triggered 1200 V solid-state circuit breakers", Proc. IEEE 3rd Workshop Wide Bandgap Power Devices Appl., pp. 162-165, 2015.

[12] Z. Gunhao, "Study on DC Circuit Breaker," 2014 Fifth International Conference on Intelligent Systems Design and Engineering Applications, Hunan, 2014, pp. 942-945, doi: 10.1109/ISDEA.2014.208.

[13] A. Shukla and G. D. Demetriades, "A Survey on Hybrid Circuit-Breaker Topologies," in IEEE Transactions on Power Delivery, vol. 30, no. 2, pp. 627-641, April 2015, doi: 10.1109/TPWRD.2014.2331696.

[14] X. Pei, O. Cwikowski, D. S. Vilchis-Rodriguez, M. Barnes, A. C. Smith and R. Shuttleworth, "A review of technologies for MVDC circuit breakers," IECON 2016 - 42nd Annual Conference of the IEEE Industrial Electronics Society, Florence, 2016, pp. 3799-3805, doi: 10.1109/IECON.2016.7793492.

[15] D. -U. Kim and S. Kim, "Modular Hybrid DC Circuit Breaker for Medium-Voltage DC System," 2020 IEEE Energy Conversion Congress and Exposition (ECCE), Detroit, MI, USA, 2020, pp. 1312-1318, doi: 10.1109/ECCE44975.2020.9235373.

[16] M. E. Baran and N. R. Mahajan, "Overcurrent Protection on Voltage-Source-Converter-Based Multiterminal DC Distribution Systems," in IEEE Transactions on Power Delivery, vol. 22, no. 1, pp. 406-412, Jan. 2007